Glück, Thorsten; Adams, Zeno

Conference Paper

Systemic Risk of Commodity Traders

Beiträge zur Jahrestagung des Vereins für Socialpolitik 2023: Growth and the "sociale Frage"

Provided in Cooperation with:
Verein für Socialpolitik / German Economic Association

Suggested Citation: Glück, Thorsten; Adams, Zeno (2023) : Systemic Risk of Commodity Traders, Beiträge zur Jahrestagung des Vereins für Socialpolitik 2023: Growth and the "sociale Frage", ZBW - Leibniz Information Centre for Economics, Kiel, Hamburg

This Version is available at:
https://hdl.handle.net/10419/277600

Systemic Risk of Commodity Traders*

Zeno Adams†, Thorsten Glück‡

January 6, 2023

Abstract

We examine the disruptions to global commodity flows following the bankruptcy of a commodity trading firm. The physical commodity network is operated by a handful of large traders that are responsible for the timely delivery of raw materials and inputs to industrial production. We propose a model that simulates the resilience and response time of the network following a shock. Our results suggest that a number of commodity traders carry significant systemic risk. The forced removal of a trader from the network has considerable implications for the prices and availability of physical commodities over a period of 6 to 12 months.

Keywords: Systemic Risk; International Trade; Commodity Trading Firms

JEL Classifications: Q40, Q41, Q43

*We would like to thank Bernd Brommundt and other oil traders at BP for valuable comments and suggestions.

†University of St.Gallen, School of Finance, Unterer Graben 21, CH-9000 St. Gallen, Switzerland; Tel.: +41 71 224 7014; E-mail address: zeno.adams@unisg.ch.

‡Corresponding author. Wiesbaden Business School, Hochschule RheinMain, DE-65183 Wiesbaden, Germany; Tel.: +49 (0) 611 94953145; E-mail address: thorsten.glueck@hs-rm.de.

1 Introduction

Commodity trading firms operate the global flow of natural resources. They are responsible for the timely delivery of primary inputs to industrial production. In this paper, we examine the question whether the failure of a commodity trading firm has systemic implications for the real economy. Systemic risk is a key research topic in financial economics that is typically associated with financial institutions. A large and mature literature has proposed a number of empirical risk measures and theoretical models which explain the economic transmission channels of systemic risk for financial firms.[1] For commodity trading firms, the systemic relevance is not obvious as these firms do not hold each other's assets on their balance sheet and do not create financial links during their operations. In contrast to financial institutions, there is thus no systemic risk within the network of commodity traders. Instead, we argue that the systemic relevance of commodity trading firms is due to their vital function as providers of raw materials to manufacturing and industrial production. Natural resource deposits are concentrated within a few countries and need to be transported by ship to the regions in which they are consumed. Commodity traders are specialist firms that manage the logistical operations of heavy, bulky, and sometimes toxic commodities. We show that the forced removal of a commodity trader from this network of physical flows can lead to a disruption of the supply chain in the buyer regions that is reflected in lower local supply and higher prices. The dynamics of this negative supply shock persist for an extended period of time. After four quarters, other traders gradually replace the missing trade routes left by the failed company.

The theoretical foundation for our paper is provided in Acemoglu et al. (2012) who study the intersectoral input-output linkages in the real economy. The key insight is the fact that when one sector acts as a supplier to chains of downstream sectors, idiosyncratic shocks to the supplier can generate cascading effects that propagate to the entire economy.[2]

[1] This literature is well summarized in the overview articles in Engle (2018) and more recently in Jackson and Pernoud (2021). Two prominent papers that contributed significantly to the literature and which are worth mentioning here are Tobias and Brunnermeier (2016) and Acharya et al. (2017).

[2] The traditional argument is that in a large and diversified economy with n producers, aggregate output volatility scales by $\sqrt{n}$. Acemoglu et al. (2012) show that under cascading effects, this might not be the case due to first- and higher order interconnections. In particular, volatility might not vanish even if $n \to \infty$.

We illustrate this mechanism for the crude oil sector in Figure 1: a commodity trader has a trading relationship with an importing region by supplying the economy of that region with natural resources such as crude oil. Crude oil is currently the number one primary energy source in the world (see, e.g., Ritchie et al., 2022) and is refined into different energy products such as road fuels, liquefied petroleum gas, and heating oil that are used in various sectors of the economy including transportation, cooking, and heating. Whether the trader occupies a central position for the buyer economy depends on how the traded goods are further processed. Inoue and Todo (2022) denote this the "upstreamness" and compare the importance of different imported products for Japan. Using a detailed data set of 4 million supply chain relationships, Inoue and Todo (2022) show that commodities such as petroleum, coal, lumber, and plastics take a central position for the economy whereas for instance transportation equipment are semi-final products that are assembled domestically. Commodity supply shocks are therefore estimated to be of larger relevance than similar shocks for other imported products.

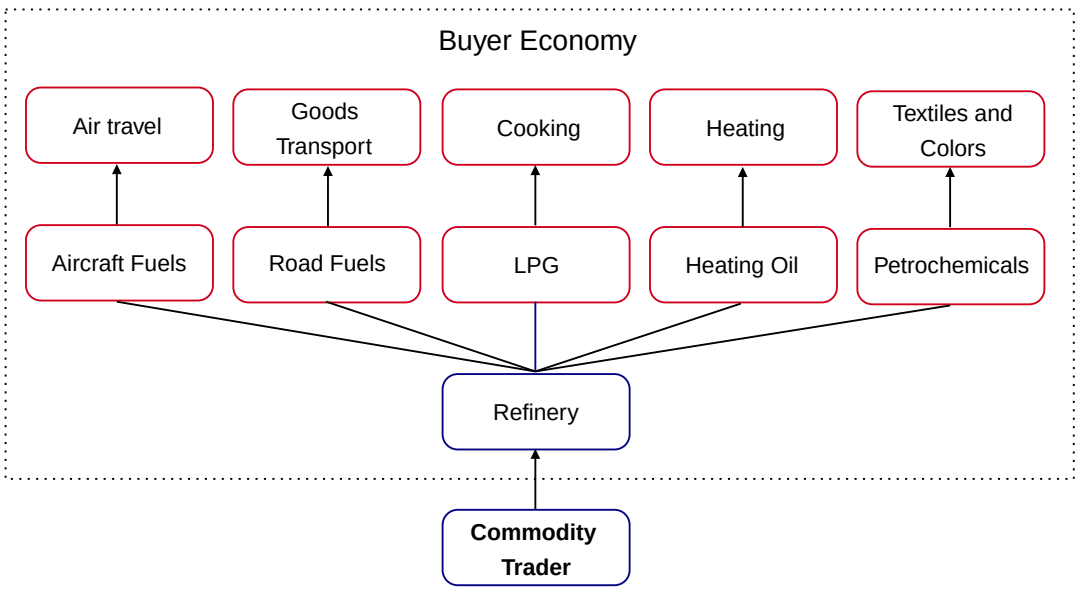

Figure 1: This figure illustrates how commodity trading firms occupy a central position in the economy's production network. Since oil is used as an input in a number of industries, the failure of the commodity trader generates a supply shock that propagates through a significant part of the real economy.

Acemoglu et al. (2012) show that in this type of setting, a disruption of the trade link that is initially idiosyncratic in nature will have systemic economy-wide effects. Hence, commodity traders are systemically relevant even for large economies if they provide raw materials that are of crucial importance for the economy's central input producers. Because of this systemic risk, we suggest to draw the attention to the possible consequences of a default of one or more of these traders. As a first step in this direction, we propose a model which allows us to simulate the dynamics of global commodity flows and prices within an adjustment period following a trader's default. We present a systemic risk ranking of commodity traders based on the simulated impact of trader default on a global as well as regional scale. Our model is based on the following economic mechanism: the default of a commodity trader causes some regions to have short-run flows that are smaller than their long-run counterparts. Local supply shortages increase commodity prices in the affected regions which in turn generate an incentive for the remaining traders to subsequently fill the gap left by the defaulted trader. Over time, equilibrium is restored as supply shortages are reduced and prices and quantities converge to their long-run values.

In order to keep our model manageable, we introduce three simplifying assumptions: First, we strictly distinguish between commodity seller and buyer regions with traders taking the role of the intermediary. There are thus no seller regions which simultaneously act as buyer regions and vice versa. Second, we assume a long-run equilibrium commodity flow matrix which determines the quantities sold from each seller to each buyer. In particular, the default of a commodity trading firm initiates a response from the remaining traders who will compensate for the local supply disruption without re-optimizing the long-term flows that are determined by this matrix. Finally, prices are the product of a global price component, a regional supply shortage margin and an additional multiplier accounting for the distance between buyer and seller region. There are hence no trader specific price components which might result from specialized knowledge or scale economies.

This basic framework of price and quantity adjustments offers three main advantages. First, our model requires the calibration of only two parameters. One parameter captures the elasticity of prices to changes in supply, the other determines the speed of the adjustment to the long-run commodity flow matrix. For the calibration of both parameters, we

can resort to existing work on commodity price shocks (see Kilian, 2014). Second, the adjustment mechanism is sufficiently general to hold for different types of commodities and in fact for all traded goods. Differences across commodities are reflected in their price elasticities and adjustment parameters. Third, in principle, we can easily incorporate trends in protectionism, deglobalisation, and other forms of effective reorganization in global trade patterns (Goldberg and Reed, 2020; Foti et al., 2013). Within our model, such changes would be reflected by defining an appropriate shift in the long-run flow matrix. For instance, the recent changes in international flows of energy commodities such as oil and gas as a consequence of the sanctions following the Russian invasion of Ukraine in 2022, can be modeled by shifting outflows from one seller region to another.[3]

We substantiate our model with data on 155,435 individual physical transactions operated by a total of 1,637 commodity trading firms. Based on annual data of seaborne oil trade from 2007 to 2018, we construct the long-run world oil flow matrix between 14 world trading zones, each comprised of a seller and buyer region. For model calibration, we utilize the flexible oil market VAR developed and applied in Baumeister and Peersman (2013a). We show that 10 commodity traders manage 43% of the global physical trade in crude oil and refined energy products, making physical trading a highly concentrated business. Using our model to simulate the failure of a commodity trading firm, we quantify the disruptions in trading flows and the resulting price impacts on exposed importing regions. The top 10 most systemically important energy firms include Unipec, Shell, BP, and Vitol. Our estimates suggest that the failure of one of these firms can lead to local supply disruptions of up to 30 million barrels per quarter and a short-term doubling in local oil prices. Given the focus of European policy makers on energy security of households and the competitiveness of energy intensive industries, these effects are economically large. In this regard, our findings also contribute to the rich literature on oil supply shocks by providing a new perspective on the possible sources of these shocks. Finally, we also provide a new perspective on systemic risk in general, which, thus far, has been dominated by the analysis of financial institutions.

[3]Our model could also be used to simulate production shocks in macroeconomic models for aggregate output (e.g. Acemoglu et al., 2012; Gabaix, 2011). Shifts in the long-run matrix and the relationship between commodity supply shocks and aggregate output, however, is beyond the scope of this paper.

The remainder of this paper is organized as follows. Section 2 provides an overview of the scant literature on the topic and discusses commodity trading firms. We propose a network model of physical commodity flows in section 3. The data on physical commodity transaction is detailed in section 4. The empirical results of our simulations are examined in section 5. Section 6 concludes.

2 Related Literature

The trading of commodity futures and its impact on commodity markets has been extensively analyzed in the academic economics literature over the past decade. The focus of this theoretical and empirical research centers primarily on the connection between pure financial investors and commodity prices as a result of the so called financialization of commodity markets (see, e.g., Basak and Pavlova, 2016; Adams et al., 2020). However, almost no attention has been paid to the market players that are eventually responsible for the physical commodity flows. In one of the few publications on this topic, Baines and Hager (2021) provide two explanations for this phenomenon. On the one hand, the majority of commodity trading firms are privately-owned. Detailed data on the physical and financial trading activities is therefore rare. Examples for such companies in private ownership are Vitol and Cargill, major players in the energy and agricultural commodity market with an annual revenue of 225bn and 113.5bn US$ in 2019, respectively (see Baines and Hager, 2021). Data availability is even more problematic in case of the many small and largely unknown trading companies (see Eggert et al., 2017). On the other hand, the analysis is complicated by the fact that there is often no clear-cut border between traditional commodity trading, i.e. connecting commodity sellers and buyers, and upstream activities such as mining or oil drilling. A prominent example is publicly held Glencore, after Vitol one of the biggest trading companies with an annual revenue of 215.1 bn US$. Glencore is nowadays heavily involved in mining activities and can be regarded as an industrial conglomerate rather than a pure trading company (Baines and Hager, 2021; Gilbert, 2021).

In this paper, we examine the most traded and most produced commodity, i.e. crude oil, with major players being traditional trading companies as well as multinational oil and gas companies such as Vitol and Shell, respectively. However, there are also a number of

other commodities for which trading is highly concentrated among a few large companies. This includes the market for cocoa analyzed by Oomes et al. (2016). Here, the four largest commodity traders, Olam, Cargill, Barry Callebaut, and Armajaro, have a market share of roughly 50% .

Our paper is also related to the literature on supply chain disruptions. Two noteworthy papers are Barrot and Sauvagnat (2016) and Carvalho et al. (2020). Both study the propagation of outside economic shocks through the supply network and the extent to which economic activity is eventually reduced. Barrot and Sauvagnat (2016) examine the impact of natural disasters such as blizzards, earthquakes, floods, and hurricanes in the United States while Carvalho et al. (2020) explore the great East Japan earthquake in 2011. The source of the shock in our paper is not generated by a natural disaster but is caused by the default of a large commodity trader. In the empirical part below, we argue that the economic size of such an event can be comparable. Finally, a recent paper that is close to our work is Inoue and Todo (2022) who study a global supply chain disruption and its impacts on a domestic economy. Inoue and Todo (2022) have a very detailed data set of 4 million supply chain relationships for Japan and show the extent to which industries are affected by the disruption. However, the source of the disruption is unspecified and related to events such as the Covid-19 pandemic.

Finally, we note that our paper is closely connected to Foti et al. (2013) who examine the integrity of the global trading network by developing a model for network dynamics and simulating different types of shocks. To a lesser extend, our paper is connected to the existing literature on commodity trading networks, e.g. Fair et al. (2017), Wei et al. (2022) and Liu et al. (2020). These studies mainly focus on pure network metrics and not, as we do here, on the possible sources and consequences of short shocks or long-run changes to the trading network.

3 Model

3.1 Trading Network

We consider an economy with K regions and N traders. The number of units of a commodity sold by a seller at region R_j to a buyer at Region R_i via trader T_n at time t is denoted by $X_{ijn,t}$. To keep the trading relationships tractable, we make the following assumption.

Assumption 1 *For any region R_j and any time t there exists at least one i, n combination such that either $X_{ijn,t} > 0$ or $X_{jin,t} > 0$. If there exists at least one i, n combination with $X_{ijn,t} > 0$, then $X_{jin,t} = 0$ for all i, n. Furthermore, for any region and any time $X_{jj,t} = 0$.*

We thus abstract from regions without any trading. At each region, there are either sellers or buyers but not both simultaneously. This assumption simplifies the analysis considerably and is consistent with our empirical analysis of the data on global trade flows in energy commodities. For instance, the regions Middle East, North Africa, and West Africa are mainly exporters of oil and refined products whereas Europe, China, and South Asia are large importing regions for oil products.[4] In general, countries or regions can be primarily regarded as sellers or buyers of a specific type of commodity. Finally, we also abstract from any trading within regions.

We consider two types of aggregation. The first type is by traders: with N traders, total commodity flows from R_j to R_i at time t are

$$X_{ij,t} = \sum_{n=1}^{N} X_{ijn,t} \tag{1}$$

Note that, on the one hand, if there exists a j with $X_{ij,t} > 0$ then $X_{ji,t} = 0$ for all i. On the other hand, for any i with $X_{ji,t} = 0$, there exists at least one j with $X_{ij,t} > 0$. The second type of aggregation is by region: total commodity inflows to region R_i at time t is obtained by aggregating over all K regions:

$$X_{i,t} = \sum_{j=1}^{K} X_{ij,t} \tag{2}$$

[4] A graphical illustration of our network of energy commodity flows is shown in Appendix C.

Again, for any region R_i, we get either $X_{i,t} > 0$ or $X_{i,t} = 0$. We call a region R_i with positive inflows, i.e. $X_{i,t} > 0$, a buyer region. Otherwise, the region is called seller region.

In the event of a bankruptcy of a commodity trader, supply shortages are expected to increase commodity prices resulting in higher import costs. For our analysis, we thus need to consider both, commodity flows and commodity prices. Let therefore $P_{ij,t}$ be the price for one unit of the commodity which has to be payed at a buyer region R_i if imported from a seller region R_j. We define this time t price as

$$P_{ij,t} = GD_{ij}M_{i,t} \tag{3}$$

where $G > 0$ is the constant global commodity price, $D_{ij} > 1$ is a constant ij specific cost multiplier, and $M_{i,t} \geq 1$ is a region R_i and time t specific margin multiplier. Multiplier D accounts for the transportation costs of shipping commodities between regions, whereas M reflects regional supply shortages.[5] Note that $P_{ij,t}$ is identical for all traders, i.e. we abstract from trader specific pricing. We also do not further elaborate how $P_{ij,t}$ is split up between traders and sellers.

The model set-up can be interpreted as a directed network with nodes and edges representing the regions and the trading relationships, respectively. There are two perspectives on this trading network: if the edges point from the seller to the buyer nodes, then the we obtain the network of physical flows and the strength of the edges are given by $X_{i,t}$. If the edges point from the buyer to the seller nodes, we obtain the network of financial flows. In this case, the strength of the edges are given by

$$C_{ij,t} = P_{ij,t}X_{ij,t} \tag{4}$$

We can interpret $C_{ij,t}$ as region R_i's time t costs of all imports from region R_j. Region R_i's total time t import costs are then given by $C_{i,t} = \sum_{j=1}^{K} C_{ij,t}$. This network interpretation is illustrated in Figure 2.

[5] In case of an oversupply, we would expect $0 < M < 1$. However, we focus on trader bankruptcies which always result in a supply shortages.

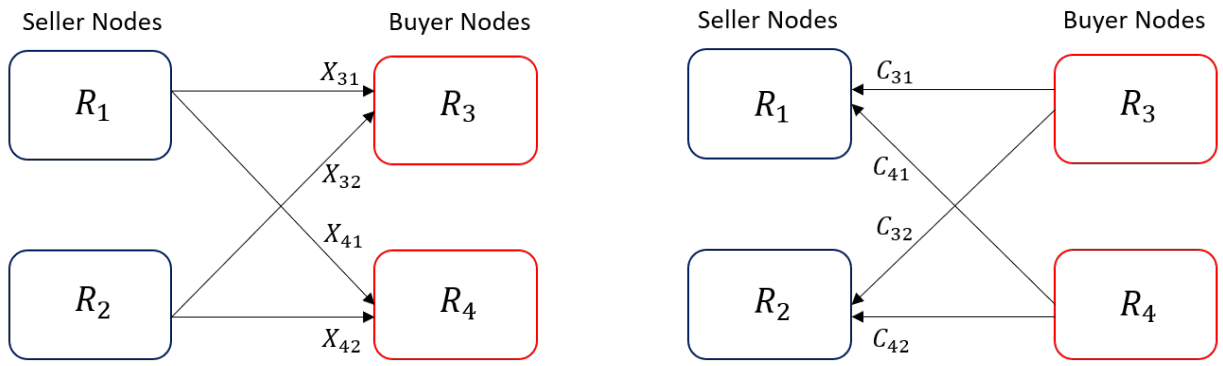

(**A**) Physical flows (**B**) Payments

Figure 2: Illustration of the commodity trading network with two seller- and two buyer nodes. The edges in panel (A) represent physical flows X. The edges in panel (B) represent financial payments $C = PX$.

3.2 Trading Dynamics

We distinguish between a long-run equilibrium and short-run adjustment dynamics. In the long-run, we assume a fixed trading relationship with fixed aggregated flows. For any buyer region R_i and seller region R_j, these long-run commodity flows are given by $\overline{X}_{ij}$. Again, to keep the model tractable, we make following simplifying assumption:

Assumption 2 *For any two regions R_j and R_i there exists a long-run commodity flow $\overline{X}_{ij} \geq 0$. The actual flows may never exceed this long-run flow, i.e. $X_{ij,t} \leq \overline{X}_{ij}$ for all t.*

We thus abstract from short run capacities above $\overline{X}$ at seller regions, which assures that there are no changes in the long-run flows.[6] This assumption is in line with real world capacity constraints. For instance, the U.S. Energy Information Administration estimates that the world surplus production capacity in the period 1973-2021 averaged 4.4 million barrels a day.[7] The majority of this capacity is generated for strategic purposes by OPEC member countries. The non-strategic surplus production capacity was only about 500,000

[6]The reason behind this requirement will become more clear in section 3.2.2 where we define the short-run adjustment process.

[7]see https://www.eia.gov/international/analysis/special-topics/Global_Surplus_Crude_Oil_Production_Capacity.

barrels a day. But even the total capacity of 4.4 million barrels a day are relatively small and comparable to half of daily U.S. shale oil production in 2021.

The structure of our model can then be outlined as follows: The long-run inflows to region R_i are $\overline{X}_i = \sum_{j=1}^{K} \overline{X}_{ij}$. These inflows balance demand and supply at R_i. Balanced supply and demand, in turn, implies a long-run margin multiplier $\overline{M}_i = 1$ and hence long-price $\overline{P}_{ij}$ and import costs $\overline{C}_{ij}$:

$$\overline{P}_{ij} = GD_{ij} \tag{5}$$

$$\overline{C}_{ij} = GD_{ij}\overline{X}_{ij} \tag{6}$$

In the short-run, we allow quantities, prices and import costs to deviate from their long-run counterparts. Let therefore t_b denote the time of a trader's bankruptcy such that $X_{i,t} < \overline{X}_i$ for at least one region R_i. The adjustment dynamics that occur afterwards are driven by a fundamental economic mechanism: due to a supply shortage at some buyer region R_i, margin multiplier $M_{i,t} > 1$ implying $P_{ij,t} > \overline{P}_{ij}$. This higher buyer region R_i price, in turn, sets an incentive for the remaining traders to fill the void left by the bankrupt trader. As the supply shortage is subsequently reduced, the import price approaches its long-run value. The margin multiplier $M_{i,t}$ returns to it's equilibrium state of 1 in which further adjustments to flows are no longer profitable for traders. The following three properties summarize this mechanism:

(*i*) If $X_{i,t} < \overline{X}_i$ then $P_{ij,t} > \overline{P}_{ij}$ for all j

(*ii*) If $P_{ij,t} > \overline{P}_{ij}$ for at least one region R_j with $X_{ij,t} < \overline{X}_{ij}$, then $X_{i,t+1} > X_{i,t}$

(*iii*) If $X_{i,t+1} > X_{i,t}$ then $P_{ij,t+1} < P_{ij,t}$ for all j

We next further specify the long-run and shock time t_b trading quantities $\overline{X}_{ij}$ and X_{ij,t_b} followed by a definition of the post-shock adjustment process for quantities and prices according to the above outlined mechanism.

3.2.1 Long-run Quantities and Trader Bankruptcy

Lets assume trader T_{n_1} declares bankruptcy at t_b. We model this scenario setting flow $X_{ijn_1,t_b} = 0$ for all i, j, n_1 combinations. This, in turn, implies $0 < X_{i,t_b} < \overline{X}_i$ for at least

one buyer region R_i. Because $\overline{X}_i$ is fixed on the long-run, the remaining traders $T_{n_2} \ldots, T_{n_N}$ have to subsequently fill the void left by bankrupt trader within post-shock period $[t_b+1, t_e]$ where $t_e > t_b$. As a result of the adjustment process outlined in the next section, for each buyer region R_i with $X_{i,t_b} < \overline{X}_i$ there is thus at least one trader $T_{n^*} \in \{T_{n_2} \ldots, T_{n_N}\}$ and one seller region R_j with $X_{ijn^*,t} > X_{ijn^*,t_b}$ for all $t > t_b + 1$.

3.2.2 Post-shock Adjustment Process

The adjustments process is comprised of two interrelated components. The first component concerns the margin multiplier as a function of supply shortages. For some $\phi > 0$, we define

$$M_{i,t} = \left(\overline{X}_i / X_{i,t}\right)^{\phi} \tag{7}$$

such that $M_{i,t} = 1$ if $X_{i,t} = \overline{X}_i$ and $M_{i,t} > 1$ if $X_{i,t} < \overline{X}_i$. According to this definition, the multiplier can be arbitrarily large. However, another, possibly more realistic definition would unnecessarily complicate the model and obscure the basic economic mechanisms. Furthermore, in our application to the commodity trading business, the supply shortage as measured by $s_i = 1 - X_{i,t}/\overline{X}_i$ does in most cases not exceed 10%, i.e. $\overline{X}_i / X_{i,t} \leq 1.11$. We discuss this issue in more detail in section 3.3.

Once converted to logs, the economic interpretation of Equation (7) is straightforward: let $m_{i,t}$, $x_{i,t}$ and $\overline{x}_i$ be the log values of $M_{i,t}$, $X_{i,t}$ and $\overline{X}_i$, respectively. Equation (7) is equivalent to

$$m_{i,t} = -\phi \Delta x_{i,t} \tag{8}$$

where $\Delta x_{i,t} = x_{i,t} - \overline{x}_i$. Let $p_{ij,t}$ and $\overline{p}_{ij}$ be the log values of $P_{ij,t}$ and $\overline{P}_{ij}$, respectively. Because $m_{i,t} = p_{ij,t} - \overline{p}_{ij}$, Equation (8) states that at some buyer region R_i, the time t relative deviation from the long-run seller region R_j price $\overline{p}_{ij}$ is $-\phi$ times the relative deviation from the respective long-run supply $\overline{x}_{i,t}$.[8] Or put differently, a decrease of the supply by $-y$ percent implies an approximate increase of the price by ϕy percent.

The second component concerns the magnitude by which the supply shortage is reduced between t and $t+1$. If $X_{i,t} < \overline{X}_i$ then $M_{i,t} > 1$ and thus $P_{ij,t} > \overline{P}_{ij}$ for all j. At a seller region R_j with buyer region R_i specific open capacities, i.e. $X_{ij,t} < \overline{X}_{ij}$, a price above

[8] Equations (5) and (3) imply $P_{ij,t} = M_{i,t}\overline{P}_{ij}$. Rearranging and taking logs yields $m_{i,t} = p_{ij,t} - \overline{p}_{ij}$.

the long-run price sets an incentive for the remaining traders to build up transportation capacities between R_j and R_i. We model this mechanism by defining

$$X_{ij,t+1} = X_{ij,t} + \kappa_{i,t} \left(\overline{X}_{ij} - X_{ij,t} \right) \tag{9}$$

where $0 < \kappa_{i,t} < 1$ is a time and buyer region specific capacity multiplier. Equation (9) states that between t and $t+1$, the seller region R_j specific part of the supply shortage at R_i is reduced by $\kappa_{i,t}$ percent. Although one could propose a number of other economically reasonable definitions for $\kappa_{i,t}$, we suggest to define for some $\psi > 0$:

$$\kappa_{i,t} = \frac{\left(M_{i,t}^{\psi} - 1 \right) X_{i,t}}{\overline{X}_i - X_{i,t}} \tag{10}$$

Note that κ depends on time-varying inputs and is therefore also time-varying while ψ is not. For any practical purpose, however, κ will be virtually constant and approximately equal to $\phi\psi$. We have outlined a more detailed description of the properties of κ in Appendix A. This definition of $\kappa_{i,t}$ has the virtue of establishing a useful and economically reasonable relationship between supply shortage, margin, and shortage reduction: inserting (10) in (9) and summing over all j yields $X_{i,t+1} = M_{i,t}^{\psi} X_{i,t}$. Summing over all sellers j aggregates to the inflows on the region level. By taking logs and rearranging, the aggregate inflows to region i can be expressed in the following intuitive form:

$$x_{i,t+1} - x_{i,t} = \psi m_{i,t} \tag{11}$$

The supply shortage is thus reduced between t and $t+1$ by approximately $\psi m_{i,t}$ percent of time t supply. For instance, taking our baseline estimates for ψ of 0.074 for quarterly data (see section 3.3) and a margin $m_{i,t}$ of 1.5, about 11% of the output gap is closed each quarter. A recent real-world example are the oil export sanctions imposed on Russia after the Ukraine invasion in 2022 which required time-intensive and costly rerouting of previously established trade links. Instead of shipping oil from the Russian ports at Primorsk or Ust Luga to Hamburg and Rotterdam within 2 weeks, oil exports are being rerouted to China which requires a round-trip voyage of 4 months.[9] As economically expected, the reduction

[9] A recent article in Forbes describes how this rerouting also requires different types of vessels that are suitable for long-distance transports. Instead of the smaller Aframax tankers that carry

increases with the level of the margin. By the following proposition, the capacity multiplier also satisfies the required restrictions. The proof is relegated to appendix A.

Proposition 1 *Let* $0 < \psi\phi < 1$. *If* $0 < X_{i,t} < \overline{X}_i$ *the multiplier* $\kappa_{i,t}$ *as defined in Equation (10) satisfies* $0 < \kappa_{i,t} < 1$.

Finally, we note that the relative deviations from the long-run supply and the long-run price exhibit an exponential decay such that these deviations approach zero with increasing time distance to the shock, i.e.

$$\Delta x_{i,t} = \Delta x_{i,t_b} (1 - \phi\psi)^{(t-t_b)} \tag{12}$$

$$m_{i,t} = m_{i,t_b} (1 - \phi\psi)^{(t-t_b)} \tag{13}$$

Given $0 < \phi\phi < 1$, the model thus yields $\overline{X}_{ij} > X_{ij,t+1} > X_{ij,t}$ and $\overline{P}_{ij} < P_{ij,t+1} < P_{ij,t}$. Furthermore, $X_{ij,t} \to \overline{X}_{ij}$ and $P_{ij,t} \to \overline{P}_{ij}$ as $(t - t_b) \to \infty$, respectively.[10] The adjustment process thus depicts the basic economic mechanism outlined in section 3.2.

3.3 Calibration for Energy Commodities

Due to our model's simplicity, we only have to set the two parameters ϕ and ψ. To obtain realistic values, we resort to the econometric literature on the impact of oil supply shocks on macroeconomic variables. This analysis is usually conducted using Vector Autoregressions (VARs). In this paper, we follow Baumeister and Peersman (2013a) and

600,000 barrels, Very Large Crude Carriers (VLCCs) that can carry 2 million barrels are needed. The shortage in vessels of this type can further prolong the shipping time which is in line with our fairly low empirical estimates (see https://www.forbes.com/sites/christopherhelman/2022/04/11/rerouting-russian-oil-would-require-dozens-of-supertankers---that-dont-exist/?sh=4c827d935446).

[10]Regarding $X_{ij,t}$, we note that Equation (12) implies $\sum_{j=1}^{K} X_{ij,t} \to \sum_{j=1}^{K} \overline{X}_{ij}$. However, because $0 < X_{ij,t} < \overline{X}_{ij}$ for all j, this convergence is only possible if each element of the sum converges to its respective long-run value, i.e. $X_{ij,t} \to \overline{X}_{ij}$. In addition, we rule out $X_{ij,t} > \overline{X}_{ij}$ even in the short run. Allowing for short-run flows above the long-run capacity would interfere with a smooth adjustment process. The margin would be negative for some seller regions while other seller regions would pause the flow adjustments. In reality, commodity supply is very inelastic in the short run and many producers have little additional output capacity so that our assumption does not appear very restrictive.

consider a VAR with time-varying parameters and stochastic volatility for the data vector $y_t = (\Delta x_t, \Delta p_t, \Delta q_t)'$, containing log differences of quarterly measures for global oil production, U.S. Crude Oil import prices and world industrial production, respectively.[11] We use this model to generate a large sample of oil supply shock induced impulse response functions (IRFs) at different hypothetical states of the economy. Estimators for ϕ and ψ are then based on these IRFs. In our model, ϕ denotes the price elasticity of the supply shock. To estimate ϕ from the data, we use the responses of oil supply and oil prices one period after a simulated oil supply shock. Regarding ψ, which measure the speed with which the quantity gap is closed, we rewrite Equations (12) and (13) as

$$\Delta x_{i,t} = \Delta x_{i,t_b} (1-\lambda)^{(t-t_b)} \tag{14}$$

$$m_{i,t} = m_{i,t_b} (1-\lambda)^{(t-t_b)} \tag{15}$$

where $\lambda = \phi\psi$. The decay rate λ is thus obtained by utilizing the responses of oil supply and oil prices for a reasonably large forecast horizon. For some given values for ϕ and λ, model parameter ψ is then simply $\psi = \lambda/\phi$. Further details regarding the VAR and the estimation of ϕ and λ from IRFs can be found in Appendix B.1 and B.2, respectively.

Our estimations indicate that 9.5 is a reasonable value for parameter ϕ, i.e. at some buyer region R_i, a decrease of the oil supply by 1% triggers an increase of the contemporary oil price by 9.5%. The estimators for the decay rate λ, in turn, range between 0.5 and 0.85. Based on these estimators for ϕ and λ, we define the three scenarios shown in Table 1.

In the first scenario, we set the optimistic values $\phi = 7.5$ and $\psi = 0.113$, i.e. a moderate impact of the supply shortage on prices and a fast adjustment to long-run supply and prices. This parameterization corresponds to $\lambda = 0.85$. In the second scenario we use $\phi = 9.5$ and $\psi = 0.074$ which implies $\lambda = 0.70$. This scenario serves as the base scenario. Finally, in the third scenario we use the pessimistic values $\phi = 11.5$ and $\psi = 0.048$, i.e. a high impact of the supply shortage an prices and slow adjustment process. In this scenario, we thus implicitly set $\lambda = 0.55$.

It should be noted that these relatively high values for ϕ correspond to a high sensitivity of the margin multiplier with respect to the supply shortage s_i. However, as we outline

[11] Examples of other VAR-based approaches are, among others, Lütkepohl and Netšunajev (2014), Kilian (2009), Kilian and Murphy (2014) and Blanchard and Riggi (2013).

	Parameter ϕ: Price Elasticity of Supply		
	7.5	9.5	11.5
Parameter ψ: Speed of Output Response			
0.048	-	-	Pessimistic Scenario
0.074	-	Base Scenario	-
0.113	Optimistic Scenario	-	-

Table 1: A combination of ϕ and ψ determines three possible scenarios for the size and length of an adjustment process following a commodity supply shock.

in detail in section 4.2, in most cases a trader's bankruptcy results in a supply shortage below 10%. Hence, $M_{i,t} \leq 2.2$ in case of the optimistic-, $M_{i,t} \leq 2.7$ in case of the base- and $M_{i,t} \leq 3.4$ in case of the pessimistic scenario (see Figure C2).[12]

As an illustration, Figure 3 shows the adjustment processes of oil supply and the oil prices for all three scenarios. For simplicity, we set $\overline{X_t} = \overline{P_t} = 1$. Between $t = 0$ and $t = 1$, the supply drops from $X_0 = \overline{X} = 1$ to $X_1 = 0.99$, i.e. by 1%. This supply shock triggers an increase of oil prices by about 8% in the optimistic scenario, 10% in the base scenario and 12% in the pessimistic scenario. In the optimistic scenario, oil supply and oil price correspond to their long-run values at $t = 3$, i.e. two quarters after the shock. In the pessimistic scenario, it takes about 6 quarters for a full adjustment. This difference in the speed of adjustment is also reflected in the difference of the capacity multipliers. In the base scenario $\kappa_t \approx \phi\psi = 0.691$, i.e. the supply shortage is reduced by approximately 69% per quarter. In contrast, in the pessimistic and optimistic scenario, we get $\kappa_t \approx 0.539$ and $\kappa_t \approx 0.848$, respectively.

[12]We note that there are a few cases with a regional supply shortage above 10%. In these cases, the shortage is capped. For more details, see section 4.2.

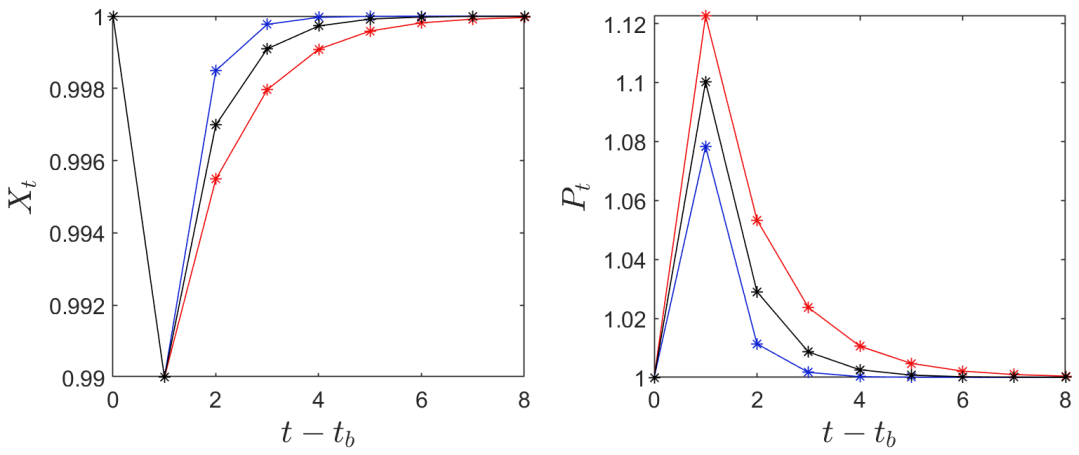

Figure 3: This figure shows the adjustment process of oil supply X and oil price P in case of the optimistic- (blue line), base- (black line) and pessimistic (red line) scenario.

4 Data

4.1 Empirical trading network

We apply our theoretical commodity network model to data on physical oil flows from Refinitiv Eikon for Commodities. This database uses a variety of sources on the individual ship level including vessel position data (AIS), port authority information, and proprietary ship to ship data. Each vessel can be tracked around the globe using it's unique International Maritime Organization (IMO) number. For instance, on January 19, 2018, the vessel "CPO LARISA ARTEMIS" with IMO number 9305532 loaded 235,538 barrels of crude oil in Slagen, Norway and shipped it to Rotterdam in the Netherlands. Later that year, we observe the same vessel load 111,424 barrels of fuel oil in Algericas, Spain to ship it to Conakry in Guinea. We track 155,435 individual flows for the years 2007 - 2018 across time and space to generate a comprehensive map of physical commodity flows encompassing 5183 ports located in 90 load and discharge zones (see Table 2).

Based on the physical flows of crude oil and refined products, we construct an empirical trading network that forms the basis of our simulation study conducted in section 5. A common approach in the trading network research literature is to focus on so called backbone networks which are simplified versions of the original networks, retaining the basic

Variable Name	Description	Values
Charterer	The commodity trading company that charters the vessel for transportation	1,637 firms
IMO number	Unique identifier for each vessel	5,454 vessels
Cargo Size	Number of barrels carried by the ship	mean: 100,501 barrels sd: 84,529 barrels
Port	Load and discharge port	5,183 ports missing values:53%
Zone	Load and discharge zone for instance U.S. Gulf, Arabian Gulf, Mediterranean	90 zones missing values:13%
Commodity Type	Crude Oil, Fuel Oil, Naphtha Gas Oil, Gasoline, Jet Fuel	-
Freight Rate	Freight rate in % of World Scale Index	mean: 113% sd: 53%

Table 2: This table summarizes the variables that are available in the Refinitiv Eikon for Commodities data set. We observe 155,435 individual shipments of energy commodities between 2007 and 2018.

network structures. Such a backbone network typically encompasses only the largest and most important trade flows, i.e. edges (see, e.g., Fair et al., 2017). For our study, we take a slightly different approach. On the one hand, we have to reduce the complexity of the empirical trading network such that it fits our theoretical model. On the other hand, due to the aim of our study, we have to keep as much trade flows for which a particular trader is responsible for as possible. As a compromise, we define a total of 15 major trading zones: 4 zones representing the Americas, 6 zones representing Europe, the Middle East and Africa (EMEA) and 5 zones representing Asia-Pacific (APAC). For each trader and each zone, we then calculate separately the average outflows and average inflows between 2007 - 2018. Aggregated flows are then obtained by summing over all traders as outlined in section 3.1. Let therefore $X_{i_1 j_2}$ be the aggregated flow from zone z_j to z_i and $X_{j_1 i_2}$ be the aggregated

flows from z_i to z_j. For simplicity, we assume that each zone is comprised of one dedicated seller region and one dedicated buyer region, to which inflows and outflows can be assigned to, i.e. z_i and z_j are comprised of buyer regions R_{i_1} and R_{j_1} and seller regions R_{i_2} and R_{j_2}. $X_{i_1 j_2}$ then represents the flow from R_{j_2} to R_{i_1} whereas $X_{j_1 i_2}$ is the flow from R_{i_2} to R_{j_1}. In line with our model, we abstract from trades within zones, i.e. $X_{i_1 i_2} = X_{j_1 j_2} = 0$.

The result of these steps is shown in Table 3. Note that trading zones with a positive net-flow are those typically regarded as oil importers, e.g. Europe, China and India, whereas trading zones with a negative net-flow are oil exporters such as the South America and the Middle East. Off course, in total, buyer region inflows match seller region outflows such that net-flows are zero. Further details regarding the sources and destinations of these flows are displayed in Figure C1.

4.2 Trader contribution

We next turn to the traders' contribution to the inflows and outflows shown in Table 3. The Gini coefficient measuring the dispersion of these trading volumes among the 1,637 traders is 0.96 which supports our claim that the commodity trading market is dominated by a relatively small number of very large traders (see also Figure C3). Even if we only consider the 100 largest traders, accounting for approximately 93% of all flows, we still get a Gini coefficient of 0.63. However, in order to make the simulation study in section 5 manageable, we further restrict the analysis to the 10 largest traders shown in Table 4. These companies account for a combined 43% of all flows.

A detailed overview of all outflows and inflows per company and region is provided in Table D1 and D2, respectively. In addition, Table D3 shows the traders' relative contributions to regional inflows. We note that in only in 10 out of 150 cases, a trader's relative contribution exceeds 10%. If we further restrict the focus to the most important buyer zones, i.e. USA, South Asia, South America, India, Europe an China, then there are only 3 cases with contributions above 10%. One reason for these very large contributions is that some traders specialize on catering to a particular region of the world. For instance, Brazil's largest oil trading firm, the state-owned Petróleo Brasileiro S.A. or "PETROBRAS" manages predominantly oil flows to Brazil. A default of PETROBRAS is therefore estimated

	Trading zone	Buyer region flow	Seller region flow	Net-flow
Americas	Canada	8.41	-2.29	6.12
	Mexico	4.47	-20.85	-16.38
	South America	17.95	-32.93	-14.98
	USA	91.81	-56.04	35.77
EMEA	East Africa	10.37	-1.13	9.25
	North Africa	3.81	-29.74	-25.93
	West Africa	12.97	-155.1	-142.13
	Europe	202.85	-56.23	146.61
	Russia	0.17	-82.9	-82.73
	Middle East	14.15	-106.53	-92.37
APAC	China	71.95	-4.64	67.31
	India	51.93	-36.13	15.8
	Japan	17.75	-2.97	14.78
	Oceania	17.93	-11.24	6.69
	South Asia	101.35	-29.15	72.2
	Σ	627.87	-627.87	0.00

Table 3: Empirical Network of physical oil flows in million barrels (MMbbl) between zones within (*i*) the Americas, (*ii*) Europe, the Middle East and Africa (EMEA) and (*iii*) Asia-Pasific (APAC). All flows are based on annual averages for a sample period ranging from 2007 to 2018.

to cause large flow reductions in Brazil, but to have little quantity effects in other parts of the world. For instance, a default of PETROBRAS is estimated to reduce oil flows to Brazil by more than 8 million barrels in the first quarter which corresponds to a reduction of approximately 45% of the total seaborne inflows in a typical quarter over the sample period. Given our estimates for the price elasticity ϕ, this would translate in very large price jumps (see Figure C2). However, a shock of this size would be likely to trigger regional land adjustment processes in which oil is transported on road and rail in an emergency

	Buyer region inflow Contribution			
Trader	Absolute	Cusum	Relative	Cusum
UNIPEC	42.35	42.35	6.75%	6.75%
SHELL	40.72	83.07	6.49%	13.23%
BP	36.33	119.40	5.79%	19.02%
VITOL	35.10	154.50	5.59%	24.61%
CNR	22.86	177.35	3.64%	28.25%
PETROBRAS	20.87	198.23	3.32%	31.57%
CSSSA	19.81	218.04	3.15%	34.73%
REPSOL	19.58	237.62	3.12%	37.85%
CLEARLAKE	16.87	254.48	2.69%	40.53%
ST SHIPPING	16.47	270.95	2.62%	43.15%

Table 4: This Table shows the absolute (in Mmbbl) and relative contribution of the 10 largest traders to aggregated average buyer region inflows. Columns 3 and 5 show the respective cumulative sums (Cusum).

response. In this paper, we concentrate on economically large but still realistic flow reductions and introduce a supply reduction cap of 10% of the long-run values. The result of this procedure in provided in Table D4 with capped inflows indicated by bold numbers.

5 Simulation of Trader Bankruptcy

The bankruptcy of a commodity trader results in the removal of that firm from the network of long-run commodity flows. We introduce a shock in period t_b that leads to a disruption of all flows operated by the defaulted trader. The impact of this shock on commodity prices in buyer region i at time $t \geq t_b$ can be measured by

$$\pi_{i,t} = \frac{P_{i,t}}{\overline{P}_i} - 1 \tag{16}$$

where $P_{i,t} = \sum_{j=1}^{K} \alpha_{ij} P_{ij,t}$ and $\overline{P}_i = \sum_{j=1}^{K} \alpha_{ij} \overline{P}_{ij}$ are weighted short- and long-run average import prices, respectively. One possibility is to use long-run imports as weights, i.e.

$\alpha_{ij} = \overline{X}_{ij}/\overline{X}_i$. However, weights are not required if we assume that $D_{ij} = D$ for all i, j which implies $P_{i,t} = GDM_{i,t}$ and $\overline{P}_i = GD$.[13] As a result, Equation (16) simplifies to

$$\pi_{i,t} = M_{i,t} - 1 \tag{17}$$

We can thus measure the vulnerability of a buyer region regarding a trader's bankruptcy via the respective margin multiplier. In the following section 5.1, we provide a ranking of the top 10 traders with respect to their system risk based on the absolute import reduction and price response π as defined in Equation (17). In section 5.2, we further analyse the dynamics π for the three scenarios provided in Table 1.

5.1 Trader Ranking

The price and quantity dynamics that unfold after the shock in the base scenario are shown in Figure 4. Panel A shows the reductions in flows over a period of 5 quarters. We consider again PETROBRAS, the large Brazilian oil trader that focuses primarily on supplying South America with energy. A default is simulated to reduce flows by a bit less than 2 million barrels, which corresponds to the number shown in Panel A and a relative supply gap of 10%. The corresponding price response shown in Panel B is economically large and estimated to be 172% in the first quarter and 35% in the second quarter. As competing oil traders reorganize to fill the flow gap of PETROBRAS, physical trade flows and prices return to pre-shock levels after the second quarter. To put the size of a 2 million barrel shock into economic perspective, we refer to simulation results from Inoue and Todo (2022) who quantify the size of import disruption on the real economy in Japan. The majority of empirical evidence on supply chain disruptions within a country is collected for Japan because the data on the industry structure of Japanese firms offers a particularly detailed

[13] Our model incorporates the more flexible buyer i and seller j specific distance measures D_{ij}. In this first approach, however, we advocate a general D as an approximation. An economic justification would be the observation that commodity demand is quite price inelastic. For instance, when export sanctions imposed on Russia led to an energy shortage in Europe, the primary objective was to procure energy at almost all costs, irrespective of the distance markup that this may entail. In addition, the notional value of the total amount of commodities carried by ship dwarf any differences in transportation costs that might arise due to geographical distance.

set of industry linkages that allow for such an analysis. Inoue and Todo (2022) estimate that a $1 import disruption from Middle Eastern countries to Japan results in a $3.12 reduction in economic production. If we assume that imports from the Middle East consist mainly of oil and that oil prices are $80 per barrel, a 2 million import reduction is worth $160m which would reduce economic production by $500m in the first quarter of the shock or 0.31% of Brazilian GDP. The joint failure of more than one large commodity trader could amplify this effect.

From Panel B we conclude that the forced removal of a commodity trader from the long run network of firms will have considerable local price effects that can extend over two quarters if the region receives the majority of imports through the defaulted trader. More generally, simulated commodity prices are more elastic than quantities, an observation that is confirmed by other studies, e.g. Baumeister and Peersman (2013a).

The price and quantity responses following the default of a commodity trading firm allows us to rank traders in decreasing order of systemic risk. Table 5 is inspired by the systemic risk ranking of financial institutions that is reported and updated by the V-Lab of New York University.[14] Our ranking reflects the impact that the default of a commodity trader exercises on both supply shortages as well as prices. The position in the overall ranking is determined by the average over both indicators. For instance, the supply shortage resulting from a default of Shell is estimated as the average weighted import reduction across all regions that receive imports from Shell over a period of 5 quarters. In particular, the default of Shell is estimated to reduce imports in the target regions United States, South Asia, and Europe on average by 9.28 million barrels per quarter. While Shell is ranked 1st in terms of supply impact, it is also estimated to have the largest price impact with prices in the three target regions estimated to be 32.6% above their long-run values that occur in the absence of any shock. While the top 10 systemically important US financial firms include names like Citigroup, JP Morgan, and Bank of America, our list features Shell, BP, and Vitol as systemically important commodity firms.

[14] See https://vlab.stern.nyu.edu/srisk

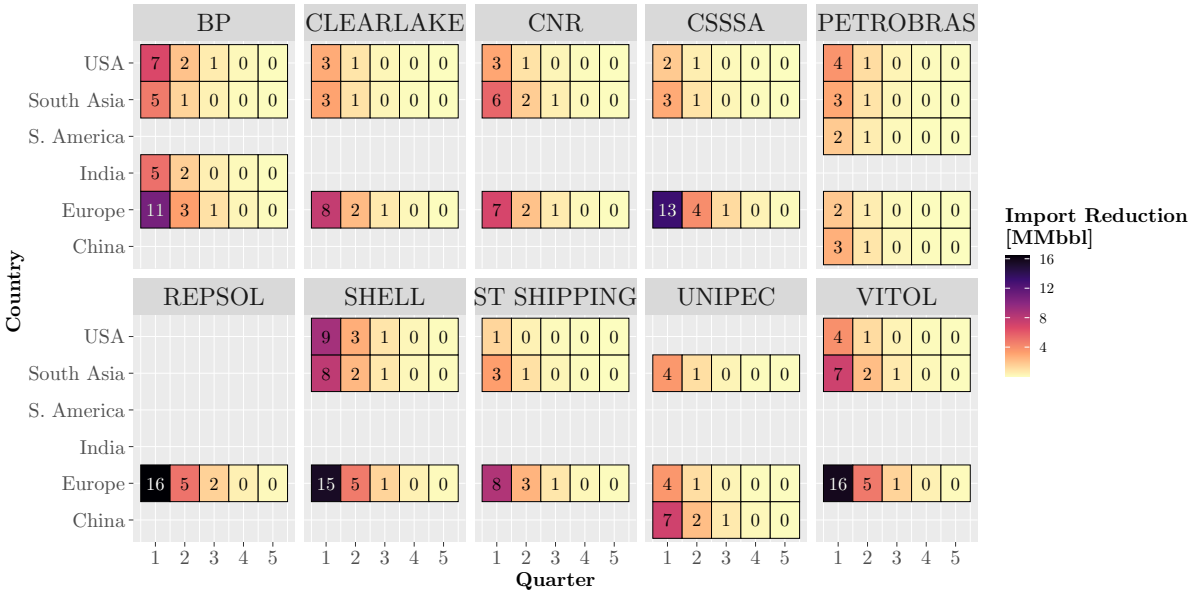

(**A**) Import Reductions

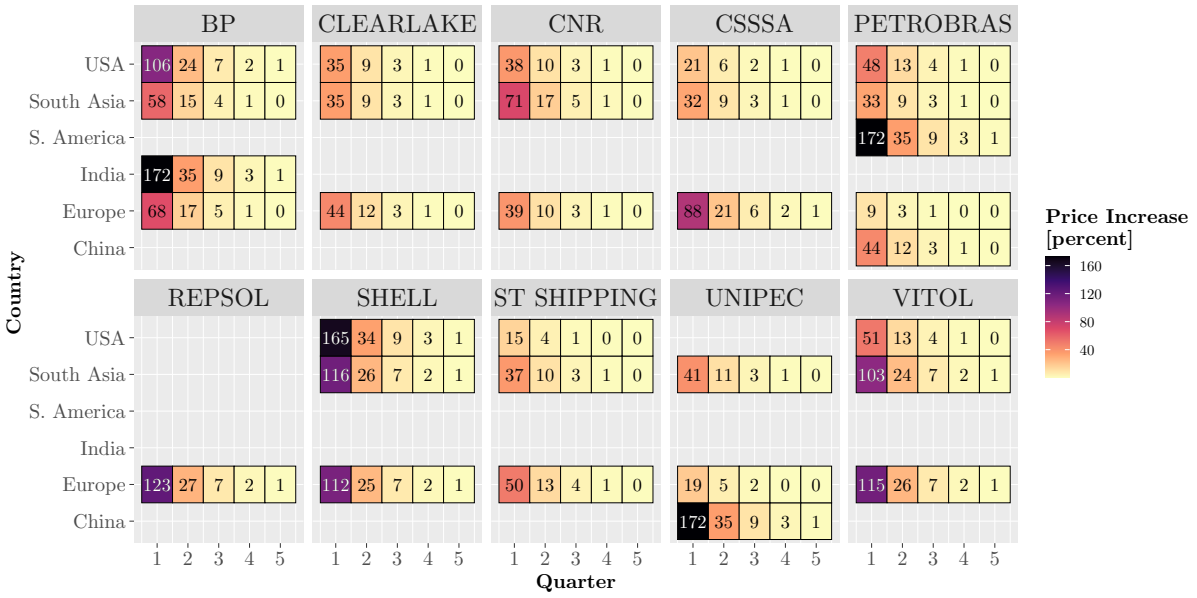

(**B**) Price Response

Figure 4: This figure shows simulated quantity and price effects following the default of a large commodity trading firm in the base scenario. Panel A highlights the regional focus of oil trading firms and the reductions in oil flows following the failure of a trader. Panel B shows the price increases that are associated with the supply disruption. Price elasticity as calibrated from data is larger than demand elasticity.

Import Reduction (in MMbbl)	**Price Impact π (in %)**	**Ranking**
9.28	32.60	SHELL
7.89	22.65	BP
7.73	25.60	VITOL
4.71	31.99	REPSOL
5.11	15.64	CSSSA
4.44	12.76	CNR
4.14	14.25	UNIPEC
3.91	10.89	CLEARLAKE
3.77	10.59	ST SHIPPING
3.74	8.86	PETROBRAS

Table 5: This table ranks the commodity trading firms in our sample according to systemic risk in the base scenario. The ranking is determined by accounting for the size in import reductions (in million barrels per quarter) and for price effects (in percent relative to equilibrium). The price averages are weighted based on flow size, i.e. buyer regions that receive higher flows also have a higher price weight.

5.2 Scenario Analysis

The import and price effects presented so far depend on price and quantity adjustment parameters in the base scenario, i.e. parameter ϕ which governs the price elasticity of a supply disruption to be 9.5 on average and λ which reflects the speed with which traders are able to respond to the resulting supply gap to be 0.7. However, the ability of the remaining traders to respond to the supply shortages left by a defaulted trader depends on the risk appetite and the funds available to take over parts of the business of the defaulted competitor. For instance, the fleet of vessels that are no longer managed by the defaulted trader requires a team of ship operators and other supporting staff in order to commence trading in the pre-shock form. Figure 5 shows three scenarios that illustrate this point.

In the optimistic scenario, the price response from the trader default, measured by the parameter ϕ, is lower than in our base scenario while the adjustment parameter λ is higher ($\phi = 7.5$ and $\lambda = 0.55$). In this optimistic scenario, the price impact is muted and supply shortages are quickly adjusted by the remaining traders. However, the circumstances in which a commodity trader goes bankrupt are likely to be financial stressful events for other remaining traders. After all, commodity traders often trade the same commodities. It is therefore quite likely that the circumstances that led to the default of a trader in the first place, reduce the funds available as well as the risk appetite of the remaining traders, which complicates the takeover of the defaulted team and can prolong the adjustment process. This case is illustrated in the pessimistic scenario in which the price response from the same shock is larger ($\phi = 11.5$) while the ability of traders to respond to the supply gap is subdued ($\lambda = 0.55$). Figure 5 therefore highlights the uncertainty that is associated with the dynamics of the shocks depending on the state and financial health of the remaining traders.

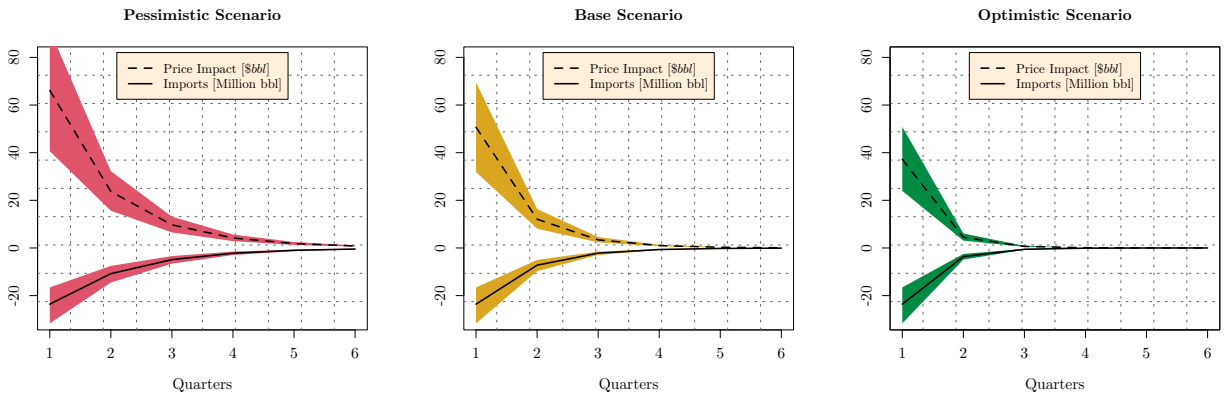

Figure 5: This figure shows post-shock import flow and price dynamics for three different scenarios. In the pessimistic scenario the supply shortage has a large price effect ($\phi = 11.5$) and the speed with which commodity traders are able to close the supply gap is low ($\lambda = 0.55$). These parameters are subsequently relaxed for the following scenarios with the optimistic scenario assuming small price jumps ($\phi = 7.5$) and flexible remaining traders who can quickly respond to the default ($\lambda = 0.85$). The solid and dashed lines are generated from weighted averages across all regions. The upper and lower bands correspond to the 75% and 25% quantile of the price and flow distribution.

6 Conclusion

Commodity trading firms are responsible for the timely delivery of energy commodities, building materials, and other natural resources that are used in the production of economic activity. A survey conducted in 2022 reports that more than half of European firms had encountered disruptions to deliveries due to shipping delays (Javorcik et al., 2022). In this paper, we argued that the failure of a commodity trader can cause supply disruptions that propagate to other sectors of the economy. In other words, commodity trading firms are systemically important. So far, commodity trading firms have shown remarkable resilience and bankruptcy is not observed in the data. We turn to simulations to address our research question. We propose a trading network model of physical commodity flows that simulates the response of the remaining traders after the bankruptcy event. Based on empirically calibrated adjustment coefficients, we estimate that the failure of one of our top ten systemically important traders has significant effects on local prices and supply. According to our estimations, regions that share trade links with the affected energy trader can experience local supply disruptions with prices doubling in the following quarter and supply cuts of up to 30 million barrels. The time dynamics following the trader bankruptcy depend on the speed of adjustment with which the remaining network of traders can accommodate the trade gap. In our pessimistic scenario that is based on the assumption that the remaining network lacks the capacity to take over major parts of the failed company, prices and supply take more than one year to return to the pre-shock equilibrium. Our results indicate that commodity trading firms might be systemically relevant but that the economic mechanism is different for commodity traders than for financial institutions. Private ownership allows commodity trading firms to operate in environments that include opaque ownership structures, unstable governments, and war zones. But it also generated an environment in which commodity traders have become systemically important without the notice of investors and regulators. Given that energy security is one of the top priorities of policy makers in Europe, our paper highlights an important mechanism that has so far been underappreciated: the systemic risk of commodity traders. Geopolitical and trade tensions force firms to reevaluate current trade relationships. A reshuffling of global supply chains can also help to mitigate the effects from disruptions due to commodity trader defaults.

Affected regions can adapt by increasing physical storage of inputs and by diversifying their base of suppliers and commodity trading firms.

References

Acemoglu, D., V. Carvalho, A. Ozdaglar, and A. Tahbaz-Salehi. (2012). The network origins of aggregate fluctuations. *Econometrica*.

Acharya, V. V., L. H. Pedersen, T. Philippon, and M. Richardson (2017). Measuring systemic risk. *The Review of Financial Studies*.

Adams, Z., S. Collot, and M. Kartsakli (2020). Have commodities become a financial asset? evidence from ten years of financialization. *Energy Economics*.

Baines, J. and S. Hager (2021). Commodity traders in a storm: financialization, corporate power and ecological crisis. *Review of International Political Economy*.

Barrot, J.-N. and J. Sauvagnat (2016). Input Specificity and the Propagation of Idiosyncratic Shocks in Production Networks. *The Quarterly Journal of Economics*.

Basak, S. and A. Pavlova (2016). A model of financialization of commodities. *Journal of Finance*.

Baumeister, C. and G. Peersman (2012). Appendix to: The role of time-varying price elasticities in accounting for volatility changes in the crude oil market. *Journal of Applied Econometrics*.

Baumeister, C. and G. Peersman (2013a). The role of time-varying price elasticities in accounting for volatility changes in the crude oil market. *Journal of Applied Econometrics*.

Baumeister, C. and G. Peersman (2013b). Time-varying effects of oil supply shocks on the us economy. *American Economic Journal: Macroeconomics*.

Blanchard, O. and M. Riggi (2013). Why are the 2000s so different from the 1970s? a structural interpretation of changes in the macroeconomic effects of oil prices. *Journal of the European Economic Association*.

Carvalho, V. M., M. Nirei, Y. U. Saito, and A. Tahbaz-Salehi (2020). Supply Chain Disruptions: Evidence from the Great East Japan Earthquake. *The Quarterly Journal of Economics 136*.

Eggert, N., G. Ferro-Luzzi, and D. Ouyang (2017). Commodity trading monitoring report. *Swiss Research Institute on Commodities*.

Engle, R. (2018). Systemic risk 10 years later. *Annual Review of Financial Economics*.

Fair, K., C. Bauch, and A. Madhur (2017). Dynamics of the global wheat trade network and resilience to shocks. *Nature Scientific Reports*.

Foti, N., S. Pauls, and D. Rockmore (2013). Stability of the world trade web overtime – an extinction analysis. *Journal of Economic Dynamic and Control*.

Gabaix, X. (2011). The granular origins of aggregate fluctuations. *Econometrica*.

Gilbert, C. (2021). Monopolistic supply management in world metals markets: How large was mount isa? *Journal of Commodity Markets*.

Goldberg, P. K. and T. Reed (2020). Income distribution, international integration, and sustained poverty reduction. Technical report, National Bureau of Economic Research.

Inoue, H. and Y. Todo (2022). Propagation of overseas economic shocks through global supply chains: Firm-level evidence. *Available at SSRN 4183736*.

Jackson, M. and A. Pernoud (2021). Systemic risk in financial networks: A survey. *Annual Review of Economics*.

Javorcik, B., L. Kitzmüller, and H. Schweiger (2022). Business unusual: Global supply chains in turbulence. Technical report, European Bank for Reconstruction and Development Transition Report 2022-23.

Kilian, L. (2009). Not all oil price shocks are alike: Disentangling demand and supply shocks in the crude oil market. *American Economic Review*.

Kilian, L. (2014). Oil price shocks: Causes and consequences. *Annual Review of Resource Economics*.

Kilian, L. and D. Murphy (2014). The role of inventories and speculative trading in the global market for crude oil. *Journal of Applied Econometrics*.

Liu, L., Z. Cao, X. Liu, L. Shid, S. Cheng, and G. Liu (2020). Oil security revisited: An assessment based on complex network analysis. *Energy*.

Lütkepohl, H. and A. Netšunajev (2014). Disentangling demand and supply shocks in the crude oil market: How to check for sign restrictions in structural vars. *Journal of Applied Econometrics*.

Oomes, N., B. Tieben, A. Laven, T. Ammerlaan, R. Appelman, C. Biesenbeek, and E. Bunk (2016). Market concentration and price formation in the global cocoa value chain. *SEO-rapport* (2016-79).

Ritchie, H., M. Roser, and P. Rosado (2022). Energy. *Our World in Data*. https://ourworldindata.org/energy.

Tobias, A. and M. K. Brunnermeier (2016). Covar. *American Economic Review*.

Wei, N., X. Wen-Jie, and Z. Wei-Xing (2022). Robustness of the international oil trade network under targeted attacks to economies. *Energy*.

Appendix A The capacity multiplier

In this section, we first provide a proof of Proposition 1, followed by a brief discussion of the behaviour of κ_t with respect to the supply shortage. In particular, we show that for supply shortages below or equal to 10%, κ_t can be approximated by $\phi\psi$.

A.1 Proof of Proposition 1

Define $\alpha = M_{i,t}^{\psi} - 1$. Because $0 < X_{i,t} < \overline{X}_i$ and $\psi > 0$ it follows that $\alpha > 0$. Recalling that $X_{i,t+1} = M_{i,t}^{\psi} X_{i,t}$, we thus get

$$X_{i,t+1} - X_{i,t} = \alpha X_{i,t} > 0 \tag{A.1}$$

Because $0 < \psi\phi < 1$, it follows by Equation (12) that $\Delta x_{i,t+1} = x_{i,t+1} - \overline{x}_i < 0$ and thus $X_{i,t+1} < \overline{X}_i$. Subtracting $X_{i,t}$ from both sides of the last inequality and substituting $\alpha X_{i,t}$ for $X_{i,t+1} - X_{i,t}$ yields

$$0 < \alpha X_{i,t} < \overline{X}_i - X_{i,t}. \tag{A.2}$$

Because $\alpha X_{i,t}/(\overline{X}_i - X_{i,t}) = \kappa_{i,t}$, dividing (A.2) by $\overline{X}_i - X_{i,t}$ yields $0 < \kappa_{i,t} < 1$ as required.

A.2 Capacity multiplier and supply shortage

It is instructive to first determine the limit that $\kappa_{i,t}$ approaches as $X_{i,t}$ approaches $\overline{X}_i$. Inserting the definition of the margin multiplier in Equation (7) into Equation (10) and rearranging yields

$$\kappa_{i,t} = \frac{\overline{X}_i^{\phi\psi} X_{i,t}^{(1-\phi\psi)} - X_{i,t}}{\overline{X}_i - X_{i,t}} \tag{A.3}$$

Because numerator and denominator approach zero as $X_{i,t}$ approaches $\overline{X}_i$, we get by l'Hospital's rule

$$\lim_{X_{i,t} \to \overline{X}_i} \kappa_{i,t} = \phi\psi$$

Having determined the limit, we next examine the deviation of $\kappa_{i,t}$ from this limit. Note that $\kappa_{i,t}$ only depends on the ratio $X_{i,t}/\overline{X}_i$. It thus suffices to show $\kappa_{i,t}$ for different values of the supply shortage which is given by $s_i = 1 - X_{i,t}/\overline{X}_i$. As outlined in section 3.3, supply shortages are limited to 10% or less. The left panel of Figure A1 plots κ against supply

shortages within this range. The dotted lines are the respective limits, i.e. $\phi\psi$. As can be seen, in all three scenarios κ is well approximated by $\phi\psi$. The right panel of Figure A1 shows the relative deviation of κ from $\phi\psi$. In all three scenarios, this relative deviation is below 2.5%.

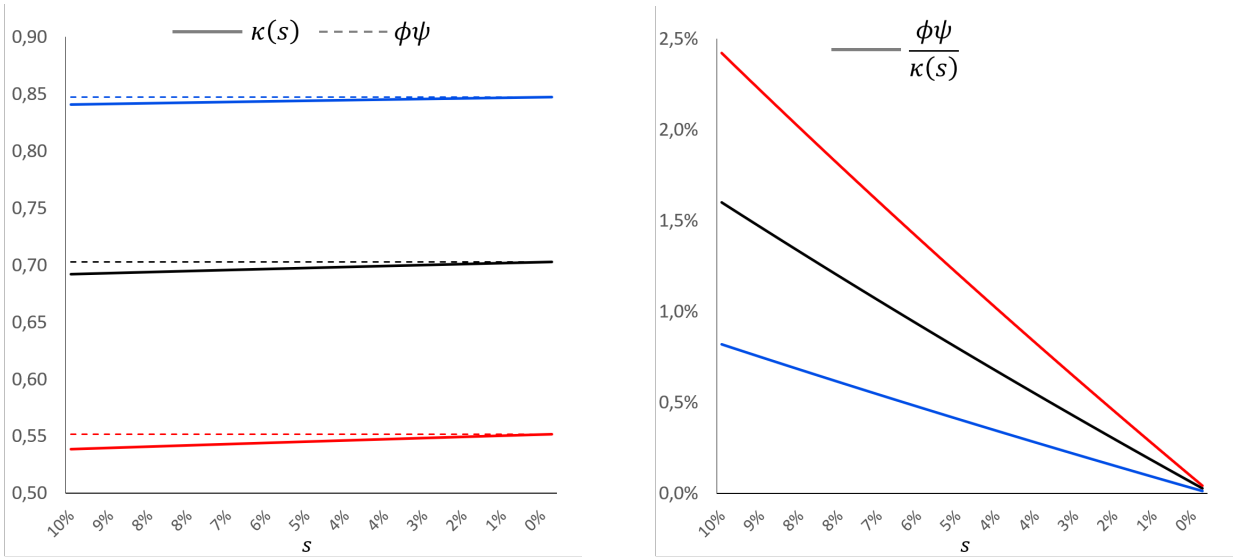

(**A**) Absolute values

(**B**) Relative deviation

Figure A1: Panel (A) shows the capacity multiplier κ as a function of the supply shortage $s = 1 - X_t/\overline{X}$. The blue line shows κ in case of $\phi = 7.5$ and $\psi = 0.113$ (optimistic scenario). The black line shows κ in case of $\phi = 9.5$ and $\psi = 0.074$ (base scenario). The red line shows κ in case of $\phi = 11.5$ and $\psi = 0.048$ (pessimistic scenario). The dotted lines are respective limits of κ given by $\phi\psi$. Panel (B) shows the corresponding relative deviations calculated as $\phi\psi/\kappa - 1$.

Appendix B Model-Parameter Estimation

B.1 VAR-Model and IRFs

Baumeister and Peersman (2013a) define a VAR(4)-model with time-varying parameters and stochastic volatility for the data vector $y_t = (\Delta x_t, \Delta p_t, \Delta q_t)'$, containing log differences of quarterly measures for global oil production, U.S. Crude Oil import prices and world industrial production, respectively. The structural form of this VAR is

$$B_{0,t}^{-1} y_t = c_t^* + \sum_{i=1}^{4} B_{i,t}^* y_{t-i} + \varepsilon_t \tag{B.1}$$

where $\varepsilon_t \sim N(0, I_3)$. Matrix $B_{0,t}^{-1}$ represents the time t instantaneous relationships between the elements of y_t. The corresponding reduced form model is

$$y_t = c_t + \sum_{i=1}^{4} B_{i,t} y_{t-i} + u_t \tag{B.2}$$

where $c_t = B_{0,t} c_t^*$, $B_{i,t} = B_{0,t} B_{i,t}^*$ and $u_t = B_{0,t} \varepsilon_t$. By assumption, $u_t \sim N\left(0, A_t^{-1} H_t (A_t^{-1})'\right)$, where A_t is a 3×3 a lower triangular matrix with ones on the main diagonal and non-zero off-diagonal elements and H_t is a 3×3 diagonal matrix. Regarding the time dependency, let $a_t = (a_{21,t}, a_{31,t}, a_{32,t})'$ be the vector containing the elements below the main diagonal of A_t, $h_t = (h_{1,t}, h_{2,t}, h_{3,t})'$ be the vector containing the main diagonal elements of H_t and $\theta_t = \text{Vec}(c_t, B_{1,t}, \ldots, B_{4,t})$.[15] The vectors θ_t and a_t are modeled as independent driftless random walks whereas $\log(h_t)$ is modeled as independent geometric random walk.

Due to its flexible structure, fitting this model to the data is somewhat more involved. Baumeister and Peersman (2013a,b) suggest to use Bayesian methods and a Markov Chain Monte Carlo Algorithm. A discussion of these methods as well as the approach to reconstruct $B_{0,t}$ is beyond the scope of this paper. For an excellent overview, we refer to Baumeister and Peersman (2012). Once model parameters are estimated, however, generating IRFs for the forecasting period $t+1$ to $t+h$ based on the relevant observations up to time t, i.e. $y_{t-3}, ..., y_t$, is straightforward and involves the following four steps:

[15] The Vec operator stacks the columns of a $m \times n$ matrix into an $mn \times 1$ vector. Here, θ_t is 39×1.

Step 1: Generate R parameter sets $\Psi_{r,t} = (\theta_{r,t+1}, ..., \theta_{r,t+h}, a_{r,t+1}, ..., a_{r,t+h}, h_{r,t+1}, ..., h_{r,t+h})$, each representing a different state of the economy from $t+1$ to $t+h$. These parameter sets are obtained by random draws from the respective estimated parameter distributions.

Step 2: For each $\Psi_{r,t}$, generate N different benchmark and shock forecast series based on $y_{t-3}, ..., y_t$ via Equation (B.2), i.e.

$\hat{y}^{(B)}_{r,n,t+1}, ..., \hat{y}^{(B)}_{r,n,t+h}$ (n'th benchmark forecast series for the r'th state)

$\hat{y}^{(S)}_{r,n,t+1}, ..., \hat{y}^{(S)}_{r,n,t+h}$ (n'th shock forecast series for the r'th state)

A difference between benchmark and shock forecasts is achieved via the reduced form innovations in Equation (B.2). In case of the benchmark series, innovations are $u^{(B)}_{t+1}, ..., u^{(B)}_{t+h}$ whereas in case of the shock series innovations are $u^{(S)}_{t+1}, ..., u^{(S)}_{t+h}$. These innovations are generated as follows: At time $t+1$, randomly draw ϵ_1, ϵ_2 and ϵ_3 from a standard normal distribution, calculate

$$u^{(B)}_{t+1} = B_{0,t+1}(\epsilon_1, \epsilon_2, \epsilon_3)' \tag{B.3}$$

$$u^{(S)}_{t+1} = B_{0,t+1}(\epsilon_1 - 1, \epsilon_2, \epsilon_3)' \tag{B.4}$$

and check following sign restrictions:

(i) $u^{(S)}_{1,t+1} - u^{(B)}_{1,t+1} < 0$ (time $t+1$ oil supply growth is lower in the shock series)

(ii) $u^{(S)}_{2,t+1} - u^{(B)}_{2,t+1} > 0$ (time $t+1$ oil price growth is higher in the shock series)

(iii) $u^{(S)}_{3,t+1} - u^{(B)}_{3,t+1} < 0$ (time $t+1$ world production growth is lower in the shock series)

If these sign restrictions are not fulfilled, generate new $u^{(B)}_{1,t+1}$ and $u^{(C)}_{1,t+1}$ and again check $(i) - (iii)$. For all $s > 1$, simulate reduced form benchmark innovations $u^{(B)}_{t+s}$ in a similar way and set $u^{(B)}_{t+s} = u^{(S)}_{t+s}$.

Step 3: For each state r, calculate the approximate conditional expectation of the time $t+1, ..., t+h$ benchmark and shock forecasts by averaging over all N values:

$$y^{(B)}_{r,t+s} = N^{-1} \sum_{n=1}^{N} y^{(B)}_{r,n,t+s} \tag{B.5}$$

$$y^{(S)}_{r,t+s} = N^{-1} \sum_{n=1}^{N} y^{(S)}_{r,n,t+s} \tag{B.6}$$

Step 4: Finally, for each state r calculate $\text{IRF}_{r,t} = (\text{IR}_{r,t+1}, ..., \text{IR}_{r,t+h})$ where

$$\text{IR}_{r,t+s} = y^{(S)}_{r,t+s} - y^{(B)}_{r,t+s} \tag{B.7}$$

We follow Baumeister and Peersman (2013a) and set $R = 500$, $N = 100$ and $h = 26$, i.e. at each t, we simulate 500 possible states of the economy, each with a oil supply shock in $t+1$ and impulse responses up to 25 quarters after the shock.[16] As an illustration, Figure B1 plots these 500 IRFs obtained for 2010-Q1. Note that $t_b = t+1$ such that $t - t_b = 0$ is the time of the shock and $t - t_b > 0$ is the post-shock period.

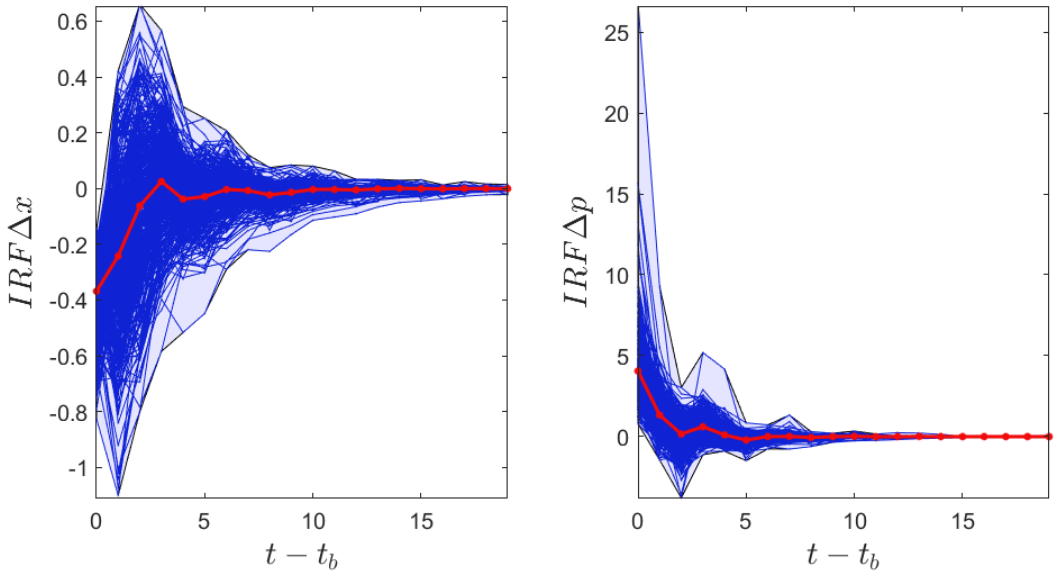

Figure B1: Simulated IRFs for 2010-Q1 (blue lines). t_b is the time of the supply shock, i.e. 2010-Q2. The red line is the average over all 500 IRFs.

[16] To estimate IRFs, we use the data set and the Matlab code provided by Baumeister and Peersman (2013a). Both is available at http://qed.econ.queensu.ca/jae/datasets/baumeister001/. Please note that we slightly adjusted the Matlab code to exclude any elasticity restrictions. For more details see Baumeister and Peersman (2013b). We also only consider the period 1972-Q1 to 2010-Q2. The original data set ranges from 1947-Q1 to 2010-Q2.

B.2 IRFs based model-parameters ϕ and ψ

We begin with parameter ϕ. Let $\text{IR}_{1,r,t+1}$ and $\text{IR}_{2,r,t+1}$ denote the first and second element of $\text{IR}_{r,t+1}$, respectively. Recall that $\text{IR}_{1,r}$ models the post-shock dynamics of oil supply while $\text{IR}_{2,r}$ denotes the price response. We obtain for the shock time $t+1$:[17]

$$\begin{aligned} \text{IR}_{1,r,t+1} &= \Delta x_{r,t+1}^{(S)} - \Delta x_{r,t+1}^{(B)} \\ &= (x_{r,t+1}^{(S)} - x_{r,t}^{(S)}) - (x_{r,t+1}^{(B)} - x_{r,t}^{(B)}) \\ &= x_{r,t+1}^{(S)} - x_{r,t+1}^{(B)} \end{aligned} \tag{B.8}$$

In a similar way, we obtain $\text{IR}_{2,r,t+1} = p_{r,t+1}^{(S)} - p_{r,t+1}^{(B)}$. If we interpret benchmark values $x_{r,t+1}^{(B)}$ and $p_{r,t+1}^{(B)}$ as proxies for the long-run values in our model, i.e. $\overline{x}_r \approx x_{r,t+1}^{(B)}$ and $\overline{p}_r \approx p_{r,t+1}^{(B)}$, we get $\text{IR}_{1,r,t+1} \approx \Delta x_{t_b}$ and $\text{IR}_{2,r,t+1} \approx m_{t_b}$. In this case, we can approximate our model equation (8) by the econometric model

$$\text{IR}_{2,r,t+1} = -\phi \text{IR}_{1,r,t+1} + e_t \tag{B.9}$$

The OLS estimator of model parameter ϕ is provided in Table B1. The estimator in the first row is based on the full set of simulated impulse responses at $t+1$, i.e. using all $R = 500$ states for all $T = 80$ observations yielding a total of 40.000 data points. The second row is based on the averaged impulse response $\text{IR}_t = R^{-1} \sum_{r=1}^{R} \text{IR}_{r,t}$ and thus only 80 data points.

Data	$\hat{\phi}$	t-Statistic
Non-averaged	9.3596	375.51
Averaged	9.9568	39.341

Table B1: OLS estimator of parameter ϕ in Equation B.9.

The estimated ϕ indicates that a 1% negative oil supply shock increase oil prices by approximately 10%. This relationship is illustrated in Figure B2 with non-averaged $t+1$ impulse responses in the left plot and averaged impulse responses in the right plot.

[17] Recall that the supply shock is in $t+1$. At pre-shock time t, we thus have $x_{r,t}^{(B)} = x_{r,t}^{(S)} = x_t$.

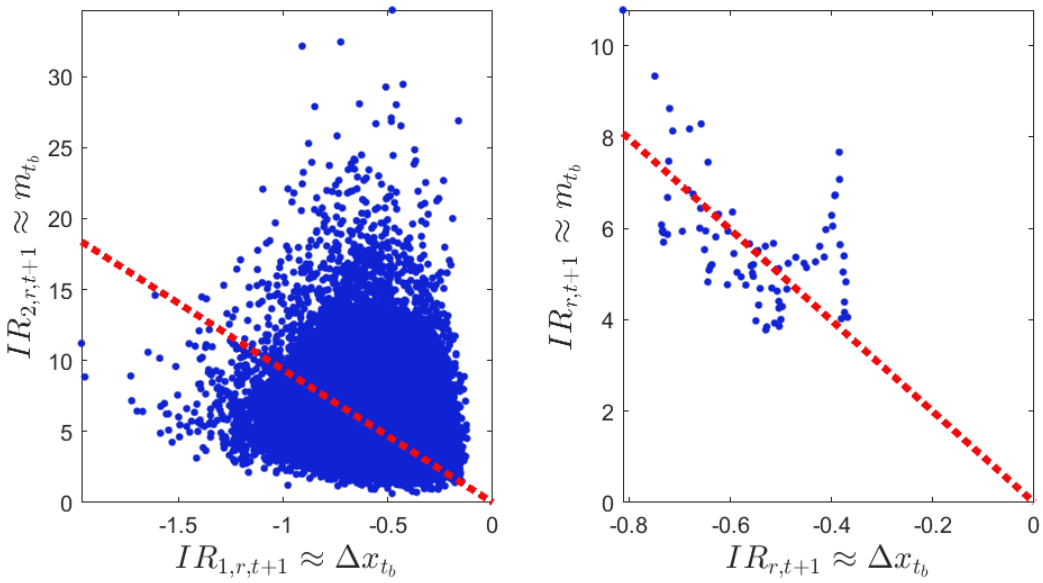

Figure B2: Impulse responses (blue dots) and estimated linear relationship (red line). The x-axis shows a change in oil production while the y-axis shows the price response which translates into a higher margin m_t. The left graph shows a total of 40,000 simulated data points while the right graph shows values that are averaged over the $R = 500$ simulations.

We next turn to the model parameter ψ which measure the extent to which a given supply shortage is reduced in the next period. Our model implies $\Delta x_{i,t} = \Delta x_{i,t_b} (1-\lambda)^{(t-t_b)}$ and $m_{i,t} = m_{i,t_b} (1-\lambda)^{(t-t_b)}$ where $\lambda = \phi\psi$. With estimators $\hat{\phi}$ and $\hat{\lambda}$ we can thus obtain an estimator for ψ via

$$\hat{\psi} = \frac{\hat{\lambda}}{\hat{\phi}} \tag{B.10}$$

All that is left is thus to get $\hat{\lambda}$. For this purpose, we define following econometric model:

$$IR_{i,r,t+s} = c_0(1-\lambda)^s + e_t \tag{B.11}$$

where $s = 0, ..., 25$ and either $i = 1$ or $i = 2$, i.e. IRs of oil supply or oil prices. By using Equation (B.11), we thus approximate the adjustment process implied by our model by the adjustment process of the shock forecasts.

As shown in Figure B1, IRs may overshoot which is ruled out by our model. For this reason, we also estimate λ for capped IRs, i.e.

$$\widetilde{\text{IR}}_{1,r,t+s} = \min\left(IR_{1,r,t+s}, 0\right) \tag{B.12}$$

$$\widetilde{\text{IR}}_{2,r,t+s} = \max\left(IR_{1,r,t+s}, 0\right) \tag{B.13}$$

The estimators of λ are shown in the second row of Table B1. Due to overshooting, non-capped IRs imply a faster adjustment than non-capped IRs. Nevertheless, all parameters imply an reasonable full adjustment within 3 to 6 quarters which is in line with the literature (see, e.g., Baumeister and Peersman 2013a). An illustration of the adjustment process is shown in Figure B2. Both plots are based on capped IRs.

	Dependent Variable			
	Oil Supply		Oil Price	
	$IR_{1,r,t+s}$	$\widetilde{\text{IR}}_{1,r,t+s}$	$IR_{2,r,t+s}$	$\widetilde{\text{IR}}_{2,r,t+s}$
Parameter				
$\hat{c}$	-0.554	-0.519	5.689	5.644
	(-49.928)	*(-64.007)*	*(51.254)*	*(70.402)*
$\hat{\lambda}$	0.854	0.505	0.741	0.570
	(44.035)	*(47.773)*	*(42.049)*	*(53.596)*

Table B2: NLS estimators of parameter λ in Equation B.11. t-statistics in parentheses.

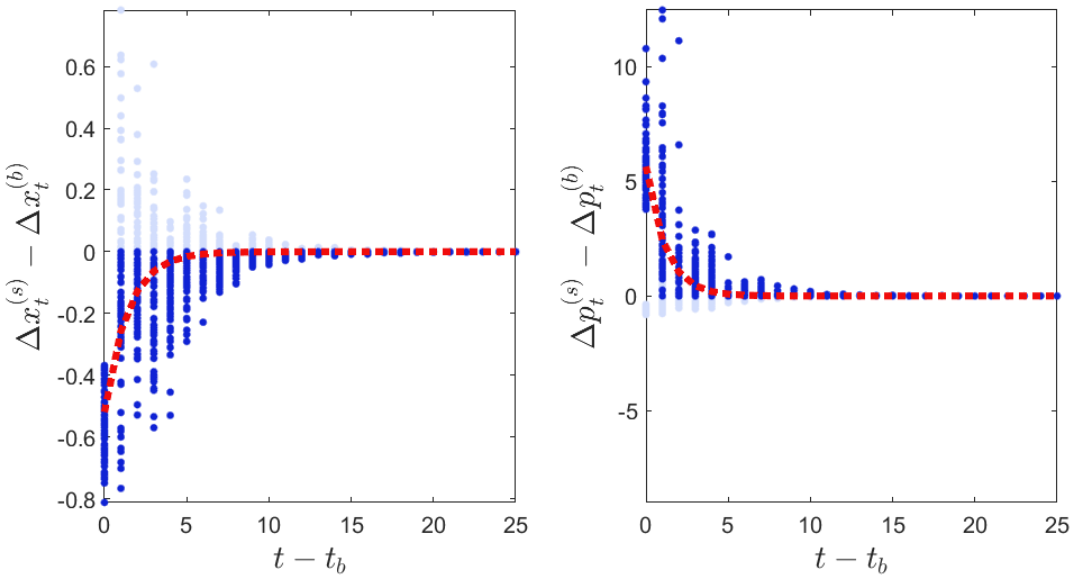

Figure B3: Impulse responses (blue dots) and estimated non-linear relationship (red dots.) The x-axis shows the time distance to the shock in t_b. The y-axis shows impulse responses of oil supply (right plot) and prices (left plot). The estimated relationship is based on Equation (B.11) with parameters provided in column 3 and column 5 of Table B2, i.e. estimators based on capped IRs as represented by the dark blue dots.

Appendix C Additional Figures and Tables

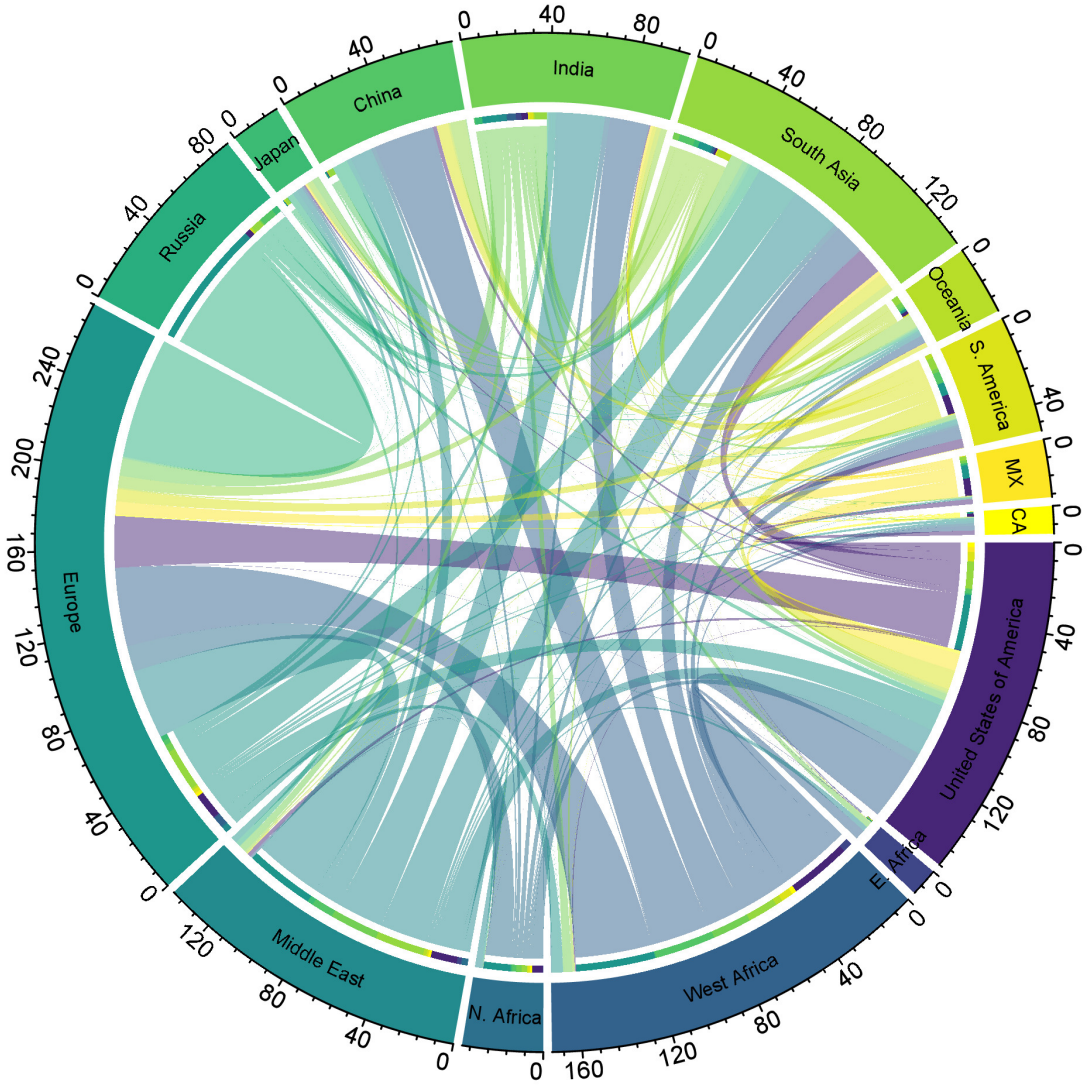

Figure C1: Empirical Network of Physical Oil Flows (2007 - 2018). This figure shows average annual flows of crude oil and refined products in million barrels. the color coding visualizes the direction of the flows. For instance, the United states is importing significant amounts of crude oil products from West Africa, the Middle East, Europe, and Mexico, but exports to Europe and South Asia.

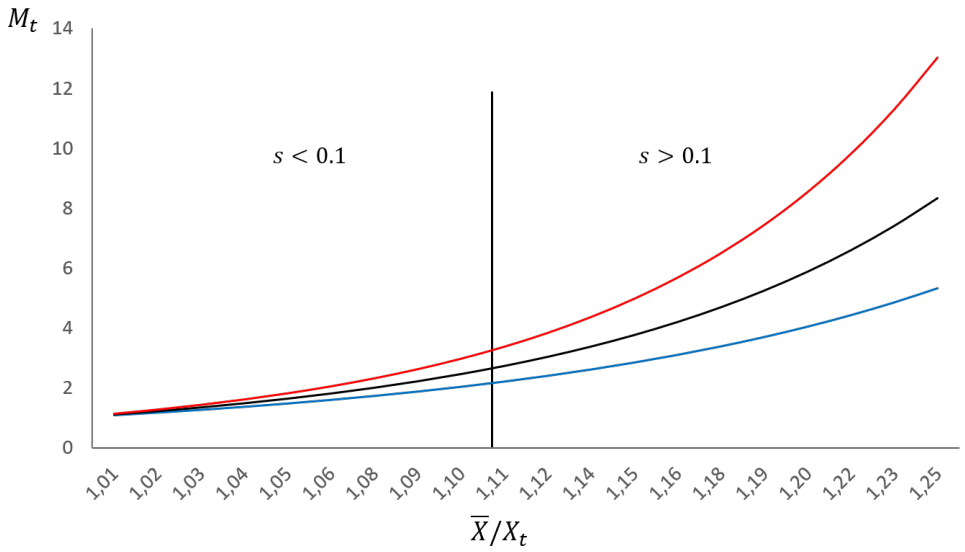

Figure C2: The x-axis of this Figure shows the ratio $\overline{X}/X_t$ while the y-axis shows the corresponding margin multiplier $M_t = \left(\overline{X}/X_t\right)^{\phi}$. The blue line shows M_t in case of $\phi = 7.5$ (optimistic scenario). The black line shows M_t in case of $\phi = 9.5$ (base scenario). The red line shows M_t in case of $\phi = 11.5$ (pessimistic scenario). Left of the vertical line, the supply shortage $s = 1 - X_t/\overline{X} < 0.1$, i.e. below 10%.

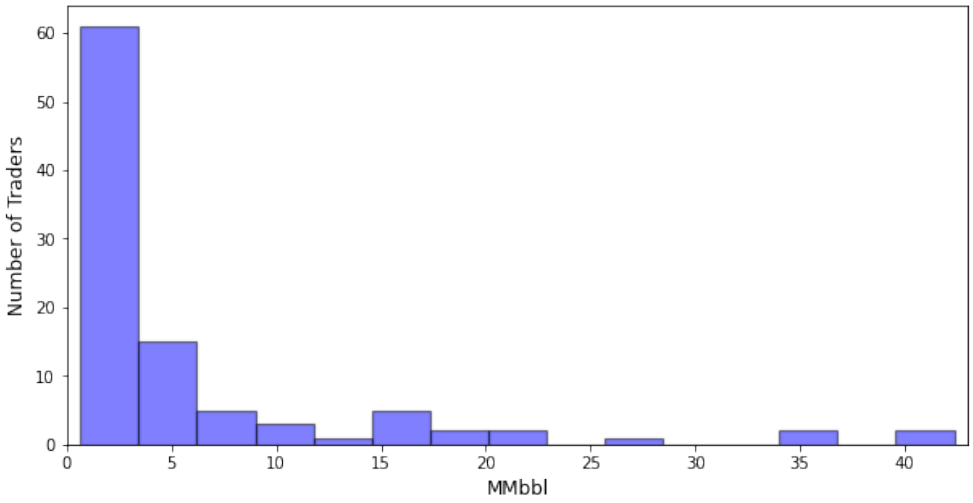

Figure C3: This figure shows the distribution of the empirical network among volumes in MMbbl across all 1,637 traders.

	UNIPEC	SHELL	BP	VITOL	CNR	PETROBRAS	CSSSA	REPSOL	CLEARLAKE	ST SHIPPING
Americas										
Canada	0.000	-0.089	-0.246	-0.027	-0.253	0.000	0.000	-0.022	0.000	-0.020
South America	-1.858	-3.686	-0.904	-0.816	-1.118	-10.638	-0.052	-1.798	-0.435	-0.194
USA	-1.846	-4.191	-3.333	-4.372	-4.806	-0.461	-2.285	-1.220	-1.813	-2.581
EMEA										
East Africa	-0.013	-0.032	-0.029	-0.059	-0.044	-0.011	-0.032	0.000	0.000	-0.020
North Africa	-1.783	-1.453	-2.235	-0.513	-0.304	-0.793	-1.225	-1.776	-0.197	-0.579
West Africa	-21.526	-9.161	-11.127	-6.261	-3.423	-5.457	-8.069	-3.184	-0.593	-2.095
Europe	-1.436	-3.106	-3.958	-3.701	-3.038	-0.668	-1.203	-0.751	-3.204	-1.083
Russia	-4.355	-7.101	-2.392	-10.087	-1.553	-0.008	-2.460	-0.806	-6.978	-5.315
Middle East	-6.499	-4.403	-4.961	-3.777	-2.305	-0.628	-2.753	-3.742	-1.389	-2.022
APAC										
China	-0.612	-0.267	-0.126	-0.227	-0.251	-0.034	-0.048	-0.022	-0.084	-0.076
India	-0.349	-2.278	-3.295	-2.011	-2.112	-1.398	-0.893	-0.022	-1.479	-1.517
Mexico	-0.440	-2.387	-0.175	-0.110	-0.446	-0.021	-0.018	-5.676	-0.017	-0.032
Japan	-0.013	-0.292	-0.146	-0.143	-0.396	-0.034	0.000	-0.007	-0.010	-0.087
Oceania	-0.200	-0.469	-0.627	-0.220	-0.341	-0.131	-0.646	-0.391	-0.081	-0.133
South Asia	-1.420	-1.803	-2.779	-2.773	-2.466	-0.594	-0.122	-0.162	-0.585	-0.714
Σ	-42.350	-40.719	-36.333	-35.096	-22.856	-20.875	-19.808	-19.579	-16.865	-16.468

Table D1: This Table shows the absolute (in Mmbbl) contribution of the 10 largest trader to average trading zone seller region outflows.

	UNIPEC	SHELL	BP	VITOL	CNR	PETROBRAS	CSSSA	REPSOL	CLEARLAKE	ST SHIPPING
Americas										
Canada	0.000	0.426	0.522	0.351	0.155	0.006	0.012	0.011	0.054	0.050
South America	0.082	0.812	0.649	0.571	0.873	8.032	0.065	1.054	0.147	0.280
USA	0.589	8.937	6.722	3.912	3.041	3.722	1.815	0.793	2.862	1.372
EMEA										
East Africa	0.007	1.065	1.605	0.338	0.215	0.006	0.373	0.046	0.056	0.191
North Africa	0.000	0.057	0.078	0.142	0.061	0.000	0.010	0.018	0.097	0.083
West Africa	0.072	0.200	0.974	1.129	1.372	0.012	0.202	0.009	0.379	0.590
Europe	3.636	15.429	10.784	15.708	6.899	1.864	13.080	16.379	7.666	8.467
Russia	0.000	0.000	0.032	0.009	0.019	0.000	0.002	0.000	0.000	0.004
Middle East	0.072	1.133	0.765	0.741	1.105	0.051	0.438	0.357	1.030	0.391
APAC										
China	33.887	1.541	0.658	1.406	1.198	2.712	0.234	0.087	0.456	0.757
India	0.025	0.427	5.396	0.174	0.207	0.666	0.137	0.019	0.166	0.244
Mexico	0.040	0.078	0.089	0.078	0.418	0.006	0.006	0.003	0.008	0.040
Japan	0.338	1.142	0.677	0.996	1.095	0.347	0.476	0.321	0.598	0.480
Oceania	0.026	1.595	2.621	2.274	0.627	0.472	0.035	0.025	0.206	0.195
South Asia	3.575	7.876	4.761	7.266	5.571	2.979	2.922	0.458	3.140	3.324
Σ	42.350	40.719	36.333	35.096	22.856	20.875	19.808	19.579	16.865	16.468

Table D2: This Table shows the absolute (in Mmbbl) contribution of the 10 largest trader to average trading zone buyer region inflows.

	UNIPEC	SHELL	BP	VITOL	CNR	PETROBRAS	CSSSA	REPSOL	CLEARLAKE	ST SHIPPING
Americas										
Canada	0.000%	5.069%	6.203%	4.178%	1.846%	0.073%	0.143%	0.126%	0.644%	0.590%
South America	0.455%	4.526%	3.615%	3.181%	4.865%	**44.748%**	0.364%	5.874%	0.818%	1.560%
USA	0.641%	9.735%	7.322%	4.261%	3.312%	4.054%	1.977%	0.863%	3.117%	1.494%
EMEA										
East Africa	0.064%	**10.268%**	**15.479%**	3.262%	2.072%	0.056%	3.597%	0.446%	0.542%	1.844%
North Africa	0.000%	1.495%	2.035%	3.738%	1.602%	0.000%	0.252%	0.468%	2.543%	2.175%
West Africa	0.559%	1.542%	7.513%	8.705%	**10.580%**	0.091%	1.558%	0.071%	2.920%	4.547%
Europe	1.792%	7.606%	5.316%	7.744%	3.401%	0.919%	6.448%	8.075%	3.779%	4.174%
Russia	0.000%	0.000%	**19.490%**	5.397%	**11.144%**	0.000%	0.900%	0.000%	0.000%	2.699%
Middle East	0.512%	8.003%	5.404%	5.238%	7.804%	0.360%	3.095%	2.523%	7.274%	2.765%
APAC										
China	**47.097%**	2.141%	0.914%	1.954%	1.664%	3.770%	0.325%	0.120%	0.634%	1.052%
India	0.048%	0.823%	**10.390%**	0.336%	0.399%	1.282%	0.265%	0.036%	0.319%	0.469%
Mexico	0.904%	1.749%	2.000%	1.754%	9.350%	0.131%	0.138%	0.069%	0.177%	0.893%
Japan	1.904%	6.434%	3.816%	5.611%	6.170%	1.957%	2.681%	1.807%	3.370%	2.704%
Oceania	0.146%	8.898%	**14.624%**	**12.685%**	3.497%	2.636%	0.195%	0.138%	1.151%	1.088%
South Asia	3.528%	7.771%	4.698%	7.169%	5.497%	2.940%	2.883%	0.451%	3.098%	3.280%

Table D3: This Table shows the relative contribution of the 10 largest trader to average trading zone buyer region inflows. Bold numbers indicate contributions above 10%.

	UNIPEC	SHELL	BP	VITOL	CNR	PETROBRAS	CSSSA	REPSOL	CLEARLAKE	ST SHIPPING
Americas										
Canada	0.000	0.426	0.522	0.351	0.155	0.006	0.012	0.011	0.054	0.050
South America	0.082	0.812	0.649	0.571	0.873	**1.795**	0.065	1.054	0.147	0.280
USA	0.589	8.937	6.722	3.912	3.041	3.722	1.815	0.793	2.862	1.372
EMEA										
East Africa	0.007	**1.037**	**1.037**	0.338	0.215	0.006	0.373	0.046	0.056	0.191
North Africa	0.000	0.057	0.078	0.142	0.061	0.000	0.010	0.018	0.097	0.083
West Africa	0.072	0.200	0.974	1.129	**1.297**	0.012	0.202	0.009	0.379	0.590
Europe	3.636	15.429	10.784	15.708	6.899	1.864	13.080	16.379	7.666	8.467
Russia	0.000	0.000	**0.017**	0.009	**0.017**	0.000	0.002	0.000	0.000	0.004
Middle East	0.072	1.133	0.765	0.741	1.105	0.051	0.438	0.357	1.030	0.391
APAC										
China	**7.195**	1.541	0.658	1.406	1.198	2.712	0.234	0.087	0.456	0.757
India	0.025	0.427	**5.193**	0.174	0.207	0.666	0.137	0.019	0.166	0.244
Mexico	0.040	0.078	0.089	0.078	0.418	0.006	0.006	0.003	0.008	0.040
Japan	0.338	1.142	0.677	0.996	1.095	0.347	0.476	0.321	0.598	0.480
Oceania	0.026	1.595	**1.793**	1.793	0.627	0.472	0.035	0.025	0.206	0.195
South Asia	3.575	7.876	4.761	7.266	5.571	2.979	2.922	0.458	3.140	3.324
Σ	15.658	40.691	34.718	34.614	22.778	14.638	19.808	19.579	16.865	16.468

Table D4: This Table shows the adjusted absolute (in Mmbbl) contribution of the 10 largest trader to average trading zone buyer region inflows. All contributions are capped at a maximum of 10% supply reduction in case of the trader's bankruptcy.